*Journal of General Virology* (2006), 87, 2859–2867 DOI 10.1099/vir.0.82128-0

# Cell target genes of Epstein–Barr virus transcription factor EBNA-2: induction of the p55α regulatory subunit of PI3-kinase and its role in survival of EREB2.5 cells

Lindsay C. Spender,[1,2]† Walter Lucchesi,[1] Gustavo Bodelon,[1,2] Antonio Bilancio,[2] Claudio Elgueta Karstegl,[1,2] Tomoichiro Asano,[3] Oliver Dittrich-Breiholz,[4] Michael Kracht,[4] Bart Vanhaesebroeck[2,5] and Paul J. Farrell[1,2]

Correspondence
Paul J. Farrell
p.farrell@imperial.ac.uk

[1]Department of Virology, Imperial College Faculty of Medicine, Norfolk Place, London W2 1PG, UK

[2,3]Ludwig Institute for Cancer Research[2] and Department of Physiological Chemistry and Metabolism[3], University of Tokyo, Tokyo 113-8655, Japan

[4]Institute of Pharmacology, Medical School Hannover, Carl Neuberg Strasse 1, D-30625 Hannover, Germany

[5]Department of Biochemistry and Molecular Biology, University College London, UK

Microarray analysis covering most of the annotated RNAs in the human genome identified a panel of genes induced by the Epstein–Barr virus (EBV) EBNA-2 transcription factor in the EREB2.5 human B-lymphoblastoid cell line without the need for any intermediate protein synthesis. Previous data indicating that PIK3R1 RNA (the α regulatory subunit of PI3-kinase) was induced were confirmed, but it is now shown that it is the p55α regulatory subunit that is induced. Several EBV-immortalized lymphoblastoid cell lines were shown to express p55α. Expression of PI3-kinase p85 regulatory and p110 catalytic subunits was not regulated by EBNA-2. Proliferation of EREB2.5 lymphoblastoid cells was inhibited by RNAi knock-down of p55α protein expression, loss of p55α being accompanied by an increase in apoptosis. p55α is thus a functional target of EBNA2 in EREB2.5 cells and the specific regulation of p55α by EBV will provide an opportunity to investigate the physiological function of p55α in this human cell line.

Received 12 April 2006
Accepted 19 June 2006

## INTRODUCTION

PI3-kinases (PI3Ks) play key roles in signal transduction from receptors for growth factors, cytokines and chemokines (Okkenhaug & Vanhaesebroeck, 2003). Class I PI3Ks are composed of a catalytic subunit (p110) and a regulatory subunit (p85, p55 or p50). It is the regulatory subunit that binds to activated growth-factor receptors, bringing the catalytic subunit in proximity to its lipid substrates; the regulatory subunit is thus required for activation of the catalytic subunit in response to growth factor-receptor activation. The conversion of PtdIns(4,5)$P_2$ to PtdIns(3,4,5)$P_3$ by PI3Ks activates signalling via the protein kinase Akt/PKB to several cell-survival mechanisms.

Three different genes give rise to the three class I catalytic subunits p110α, -β and -δ. The p85α, p55α and p50α regulatory subunits are all derived from the same gene (PIK3R1). Different transcription promoters express the separate first exons of p85α, p55α and p50α, which are then spliced to common additional exons to make the complete mRNAs. The C-terminal protein sequences of p85α, p55α and p50α are therefore identical, but each has a unique N terminus (Fig. 1a). Separate genes express the other regulatory subunits, p85β and p55γ. The expression and function of PI3Ks in lymphocyte development, differentiation and activation have recently been reviewed in detail by Okkenhaug & Vanhaesebroeck (2003).

Epstein–Barr virus (EBV) is a human herpesvirus that infects most people in the world and is involved in several types of cancer (Kieff & Rickinson, 2001). Infection of primary resting human B lymphocytes by EBV induces cell proliferation very efficiently, and lymphoblastoid cell lines (LCLs) are readily grown out in culture. In LCLs, the virus exhibits a latent infection, expressing only 11 of the viral genes, including the EBNA-2 gene. By replacing the EBNA-2

†Present address: Growth Factor Signalling Laboratory, The Beatson Institute for Cancer Research, Garscube Estate, Switchback Road, Bearsden, Glasgow G61 1BD, UK.

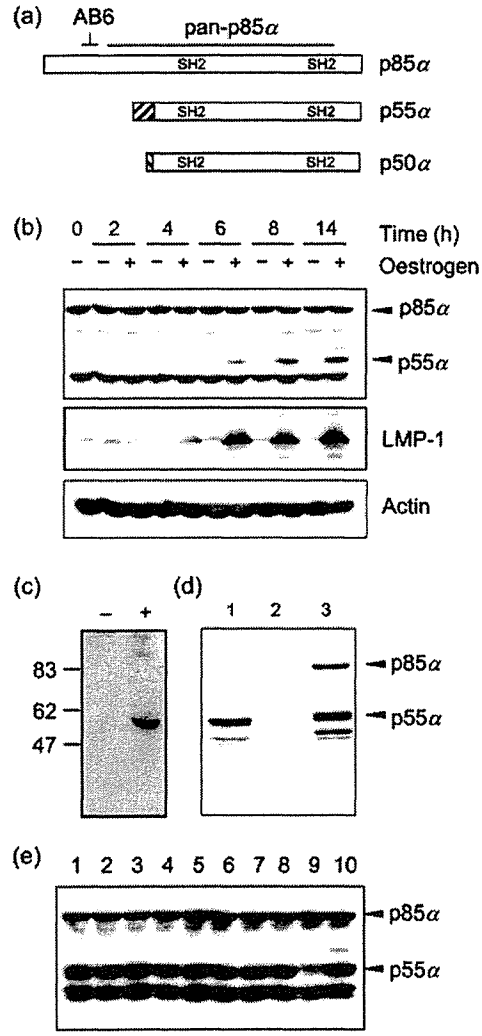


**Fig. 1.** (a) Schematic alignment of the regulatory subunits encoded by the PIK3R1 gene. Epitopes recognized by the antibodies AB6 and pan-p85α are shown. The unique first exons of p55α and p50α are hatched and the SH2 domains in the common parts of the proteins are marked. (b) Kinetics of p55α induction in EREB2.5 cells reactivated by β-oestradiol addition to the medium of cells after withdrawal of β-oestradiol for 5 days. Samples (50 μg) of cell lysate were analysed by SDS-PAGE and immunoblotting for the EBNA-2-induced EBV protein LMP-1 and for the PIK3R1 regulatory subunits by using a pan-p85α antibody and actin as a loading control. (c) Western blot of EREB2.5 cells with or without β-oestradiol treatment with anti-p55α-specific antibody. (d) *In vitro*-translated p55α co-migrates in SDS-PAGE with p55α in EREB2.5 cells. Western blot was carried out by using pan-p85α antibody. Lane 1, *in vitro*-translated p55α; lane 2, *in vitro* translation negative control; lane 3, EREB2.5 cell extract. (e) EREB/E2 cells (lanes 1–8) growing independently of β-oestradiol were assayed by immunoblotting with pan-p85α antibody. Lane 9 shows extract from LCL-C (a B95-8 LCL that has a very low level of p55α) and lane 10 is EREB2.5 cells stimulated with β-oestradiol for 14 h as a positive control.

gene of EBV with a conditionally active oestrogen receptor (ER)–EBNA-2 fusion gene, the EREB2.5 cell line (Kempkes *et al.*, 1995) was created to investigate the function of EBNA-2 in the context of a normal EBV infection. Continued activity of EBNA-2 was shown to be essential for proliferation of LCLs (Kempkes *et al.*, 1995). The EBNA-2 protein is a transcription factor that coordinates latent viral gene expression and induces several cellular genes that are important for proliferation, including c-MYC and RUNX-3 (Kaiser *et al.*, 1999; Spender *et al.*, 2002, 2005). Our previous microarray expression profiling that identified EBNA-2 target genes in EREB2.5 cells reported induction of the p85α mRNA, but no change in p85α protein was detected in response to EBNA-2 (Spender *et al.*, 2002). Use of protein-synthesis inhibitors in those experiments demonstrated that no intermediate protein expression was required between EBNA-2 and induction of the PIK3R1 mRNA.

Early studies using wortmannin to inhibit PI3K activity indicated a role for these enzymes in the immortalization of primary human B cells by EBV (Sinclair & Farrell, 1995). The PI3K inhibitor LY294002 was subsequently shown to prevent growth of established LCLs, causing an accumulation of cells in the G1 phase of the cell cycle (Brennan *et al.*, 2002). Signal-transduction effects of EBV proteins on PI3K activity are thought to be mediated mainly by EBV LMP-2A and LMP-1. The LMP-2A protein can mediate B-lymphocyte or epithelial-cell survival through activation of the PI3K pathway (Fukuda & Longnecker, 2004; Portis & Longnecker, 2004; Scholle *et al.*, 2000; Swart *et al.*, 2000) and LMP-1 can also activate PI3K to promote cell survival and induce actin-filament remodelling (Dawson *et al.*, 2003). As the LMP1 and LMP-2A genes are induced directly by EBNA-2 in EBV LCLs, signal transduction from LMP-1 and LMP-2A to PI3Ks is controlled indirectly by EBNA-2. In contrast to that signal-transduction control, in this paper we focus on the direct regulation of expression of a specific PI3K regulatory subunit by EBNA-2.

Here, we show that it is in fact the p55α regulatory subunit of PI3K that is induced by EBNA-2 in EREB2.5 cells, not p85α. Not all EBV-infected cell lines have p55α expression, but RNA interference (RNAi) of the p55α subunit in EREB2.5 cells reduces proliferation and is accompanied by apoptosis. The regulation of p55α expression by EBNA-2 thus provides a valuable and novel system to study the physiological regulation of expression of this PI3K regulatory subunit in human cells.

## METHODS

**Cell culture.** All LCLs were maintained in RPMI 1640 medium (Gibco-BRL) supplemented with 10–15% (v/v) heat-inactivated fetal calf serum and antibiotics. EREB2.5 cells (Kempkes *et al.*, 1995) contain a conditional EBNA-2 protein regulated by oestrogen and were maintained in RPMI 1640 medium without phenol red (Gibco-BRL) supplemented with 10% heat-inactivated fetal calf serum, antibiotics (100 U penicillin $ml^{-1}$ and 100 μg streptomycin $ml^{-1}$) and 1 μM β-oestradiol. For oestrogen-withdrawal experiments, cells were washed twice in serum-free medium before being

resuspended at $5 \times 10^5$ ml$^{-1}$ in phenol red-free RPMI 1640 medium without β-oestradiol. Cells were then incubated for 5 days prior to EBNA-2 induction by addition of 1 μM β-oestradiol. β-Oestradiol-independent cell lines (EREB/E2) were also generated from EREB2.5 cells by Amaxa transfection with the p554 plasmid expressing wild-type EBNA-2 (Kempkes *et al.*, 1995). These cells were selected for growth in the absence of β-oestradiol.

**Microarray analysis.** Microarray analysis was conducted on Agilent G4122A 44K HD arrays using total RNA from EREB2.5 cells. Cells were starved of oestrogen, then oestrogen was added back in the presence of protein-synthesis inhibitors and cells were harvested 4 h later as in our previous studies (Spender *et al.*, 2002). RNA preparations from cell cultures with and without oestrogen were transcribed into Cy3- or Cy5-labelled cRNA, respectively, and cohybridized onto the same microarray. Samples derived from three independent experiments were analysed separately on three arrays, including one dye-swap experiment. Arrays were scanned on an Affymetrix 428 instrument and data were extracted by using Imagene 5.0. The values were filtered for genes that showed regulation by at least twofold in each individual experiment. The results were curated for flagged spots and for probes without GenBank accession number and were expressed as a ratio of values plus oestrogen divided by values minus oestrogen. The mean and SD are shown in Table 1. Several of the genes identified were represented on the array multiple times and these values have been included in the computation of the mean and SD.

**Immunoblotting and antibodies.** RIPA cell lysates were prepared by using cell lysis buffer (Cell Signaling Technology) and protein concentration was determined. Proteins were fractionated by SDS-PAGE and transferred to a nitrocellulose membrane. After blocking with 10% milk powder in 140 mM NaCl, 10 mM Tris/HCl (pH 7·7) and 0·05% Tween 20, the membranes were probed with the following antibodies. A 1/10 dilution of anti-LMP-1 mouse monoclonal S12 (Mann *et al.*, 1985) was used; anti-EBNA-2 (PE-2; Dako) was used at 1/500. Antibodies specific for cleaved PARP (Asp 214) were from Cell Signaling Technology. Anti-PIK3R1 p85α (06-195 rabbit antiserum; Upstate) is a pan-p85α antibody recognizing p85α, p55α and p50α and was used at a final concentration of 1 μg ml$^{-1}$. Antisera to p110α (1/250), p110β (1/2000) and p110δ (1/5000) (Ali *et al.*, 2004), anti-p55α (1/1000) and anti-p55γ (Inukai *et al.*, 1996) and p85α-specific antibody U2 (End *et al.*, 1993) have been described previously. Anti-p85β (T15, ab252) was from Abcam and the mouse monoclonal anti-β-actin (AC-15; Sigma) was used at 1/10 000. The secondary antibodies were horseradish peroxidase (HRP)-conjugated goat anti-rabbit immunoglobulin (Ig) (Dako), peroxidase-conjugated rabbit anti-rat (Sigma) and HRP-conjugated sheep anti-mouse Ig (Amersham Biosciences). Bound immunocomplexes were detected by enhanced chemiluminescence (ECL; Amersham Biosciences).

***In vitro* translation.** *In vitro* translation was carried out by using a Mammalian Gene Collection (MGC) clone containing the cDNA for p55α (GenBank accession no. BC030815). *In vitro* translation was performed by using 1 μg plasmid linearized with *Xba*I in the TNT T7 coupled wheatgerm extract system (Promega).

**[$^3$H]Thymidine-incorporation assay.** Cells were seeded at a density of $5 \times 10^4$ per well in 96-well plates and were pulse-labelled for 2 h with 1 μCi (37 kBq) [$^3$H]thymidine per well before being harvested onto glass-fibre filters with a cell harvester (Skatron Ltd). The amount of [$^3$H]thymidine incorporated into DNA was measured by scintillation counting and the results were displayed as the mean and SD of at least three separate determinations.

**Co-immunoprecipitation assay (IP).** PI3K regulatory and catalytic subunits were immunoprecipitated from cell lysates after pre-clearing with protein A–Sepharose (Amersham Biosciences). Cell lysate was mixed overnight at 4 °C with 1 μg antibody or 1 μg control Ig. Protein A–Sepharose was added for 3 h at 4 °C to bind the immunocomplexes. The Sepharose was washed three times in lysis buffer followed by two washes with PBS before being pelleted and resuspended in SDS sample buffer. The solution was heated to 95 °C for 5 min, the Sepharose was pelleted and the supernatant was analysed by SDS-PAGE and Western blotting.

**RNase-protection assay (RPA).** In RPA experiments to identify direct targets of EBNA-2 transcription, protein synthesis was inhibited by pre-treating oestrogen-starved EREB2.5 cells for 2 h with 50 μg cycloheximide ml$^{-1}$ and 100 μM anisomycin (Sigma) prior to the addition of oestrogen. Total cellular RNA was extracted by using RNAzol B (Biogenesis) and quantified by measuring $A_{260}$. An RPA probe for detection of p55α RNA was generated by PCR from human genomic DNA using the primers 5′-TTTTCTGACTTGATTGGCTGGG-3′ and 5′-CAGTATTACCTGGTGGGTCCATTTC-3′ to generate a protected fragment of 168 bp. The PCR product was cloned into pCR2.1-TOPO, sequenced and subcloned into pBS II SK. A $^{32}$P-labelled antisense RNA RPA probe was then generated by using T7 RNA polymerase in *in vitro* transcription of 1 μg plasmid DNA linearized with *Not*I. RPAs were performed by using an RPA III RNase protection assay kit (Ambion). Cellular RNA was hybridized overnight at 42 °C with 50 000 c.p.m. probe. An equivalent amount of yeast RNA was included in a hybridization reaction as a negative control. Single-strand RNA was digested with an RNase A/T1 mixture for 30 min at 37 °C. Protected fragments were precipitated, fractionated on a polyacrylamide gel and the sizes were compared with $^{32}$P-labelled, *Msp*I-digested pBR322 markers. The gel was analysed on a phosphorimager.

**Generation of p55α short interfering RNA cells.** Oligonucleotides were cloned into pHEBo-SUPER (Spender *et al.*, 2005) and plasmid DNA was Amaxa electroporated into EREB2.5 cells. Transfected cells were grown in 150 μg hygromycin ml$^{-1}$ (400 μg ml$^{-1}$ for the first 3 days) and viable cell numbers were determined 12 days later. Samples were also taken for Western blotting for p55α expression. The p55α oligonucleotides cloned for RNAi were 5′-GATCCCCGACCTGGATTTAGAATATGTTCAAGAGACATATTCTAAATCCAGGTCTTTTTA-3′ and 5′-AGCTTAAAAAGACCTGGATTTAGAATATGTCTCTTGAACATATTCTAAATCCAGGTCGGG-3′.

## RESULTS

### EBNA-2 target genes using whole-genome arrays

Our previous microarray expression profiling of EBNA-2 target genes used arrays that only represented about 9000 human genes, so we have extended the same experiment to larger arrays that represent most of the annotated genes in the human genome. This produced an extended list that included all of our previously identified targets (Table 1). These genes are direct targets of EBNA-2 regulation in the sense that no intermediate protein synthesis is required for the induction of their RNAs. In Table 1, the list is truncated arbitrarily at about twofold induction and genes with no annotated function have been omitted. Notable novel genes in the list include members of the Notch signalling pathway (HES1, HEY1 and DTX1), the secreted DNase 1L3, a protein phosphatase (PPEF1), various chemokines, an orphan receptor CMKOR1 and the Ets-1 transcription factor. The complete list of regulated genes is available from the authors

**Table 1.** List of genes upregulated directly by EBNA-2, ranked by fold induction

Ratio is mean of values plus oestrogen divided by values minus oestrogen; SD is standard deviation. The list is truncated arbitrarily at about twofold induction and RNAs with no annotated function have been omitted. A complete list is available from the authors.

| Description | Symbol | Ratio | SD |
|---|---|---|---|
| Chemokine orphan receptor 1 | CMKOR1 | 17·09 | 5·60 |
| C-MYC | MYC | 16·57 | 3·51 |
| DNASE1L3 | DNASE1L3 | 15·88 | 7·33 |
| Hairy/enhancer of split | HES1 | 11·71 | 1·40 |
| Abhydrolase domain-containing 6 | ABHD6 | 10·77 | 2·45 |
| Protein phosphatase, EF-hand calcium-binding domain 1 | PPEF1 | 10·08 | 2·87 |
| Chitinase 3-like 2 | CHI3L2 | 7·53 | 1·46 |
| Hairy/enhancer of split-related with YRPW motif 1 | HEY1 | 7·01 | 3·53 |
| Endothelial differentiation, sphingolipid G protein-coupled receptor | EDG1 | 6·61 | 2·66 |
| Dynamin-binding protein | DNMBP | 6·17 | 0·92 |
| CR2/CD21 | CR2 | 5·69 | 1·19 |
| T-cell co-stimulator | ICOS | 5·39 | 0·43 |
| Phosphoinositide-3-kinase, regulatory subunit PIK3R1 | PIK3R1 | 5·23 | 0·89 |
| Germinal centre-expressed transcript 2 | GCET2 | 5·21 | 0·69 |
| Interleukin-1 receptor, type II | IL1R2 | 4·16 | 2·14 |
| Chemokine (C–C motif) ligand 3 | CCL3 | 4·06 | 0·76 |
| Deltex homologue 1 | DTX1 | 4·03 | 0·75 |
| Chemokine (C–C motif) ligand 3-like 3 | CCL3L3 | 4·00 | 0·89 |
| Retinoschisis (X-linked, juvenile) 1 | RS1 | 3·99 | 0·81 |
| ETS1 transcription factor | ETS1 | 3·98 | 1·29 |
| Guanine nucleotide-binding protein (G protein) | GNGT2 | 3·94 | 0·68 |
| Cyclin-dependent kinase-like 5 | CDKL5 | 3·90 | 0·16 |
| Growth arrest and DNA damage-inducible, beta | GADD45B | 3·72 | 0·30 |
| Phosphoinositide-3-kinase adaptor protein 1 (BCAP) | PIK3AP1 | 3·60 | 0·30 |
| CD84 | CD84 | 3·55 | 0·15 |
| Prickle-like 1 | PRICKLE1 | 3·45 | 0·23 |
| Interferon-induced protein with tetratricopeptide repeats 2 | IFIT2 | 3·42 | 0·54 |
| FERM domain-containing 4A | FRMD4A | 3·41 | 0·11 |
| DNA damage-inducible transcript 4 | DDIT4 | 3·39 | 1·07 |
| Interferon regulatory factor 4 | IRF4 | 3·20 | 0·40 |
| Geminin, DNA replication inhibitor | GMNN | 3·19 | 1·15 |
| EH-domain containing 1 | EHD1 | 3·17 | 0·78 |
| *Homo sapiens* formin-binding protein 1 | FNBP1 | 3·16 | 0·23 |
| EBI2 (lymphocyte-specific G protein-coupled receptor) | EBI2 | 3·16 | 0·24 |
| GTPase, IMAP family member 1 | GIMAP1 | 3·13 | 1·30 |
| Neural precursor cell-expressed, developmentally downregulated 9 | NEDD9 | 3·13 | 0·41 |
| Cadherin 1, type 1, E-cadherin | CDH1 | 2·95 | 0·36 |
| Ectodermal-neural cortex (with BTB-like domain) | ENC1 | 2·92 | 0·33 |
| Chemokine (C–C motif) receptor 7 | CCR7 | 2·90 | 0·32 |
| Interleukin 16 (lymphocyte chemoattractant factor) | IL16 | 2·88 | 0·58 |
| *Homo sapiens* chemokine (C–C motif) ligand 4 (CCL4) | CCL4 | 2·82 | 0·53 |
| Solute carrier family 1 (glutamate/neutral amino acid transporter) | SLC1A4 | 2·79 | 0·14 |
| Interferon-induced protein with tetratricopeptide repeats 3 | IFIT3 | 2·76 | 0·49 |
| Protein tyrosine phosphatase type IVA, member 3 | PTP4A3 | 2·76 | 0·80 |
| Achaete-scute complex-like 1 | ASCL1 | 2·74 | 0·26 |
| HECT, C2 and WW domain-containing E3 ubiquitin protein ligase 2 | HECW2 | 2·71 | 0·35 |
| ATPase, $Na^+/K^+$-transporting, beta 1 polypeptide | ATP1B1 | 2·68 | 0·50 |
| CD300A antigen | CD300A | 2·63 | 0·57 |
| Transmembrane protein 2 | TMEM2 | 2·61 | 0·45 |
| Purinergic receptor P2X, ligand-gated ion channel, 5 | P2RX5 | 2·60 | 0·32 |
| RUNX3, Runt-related transcription factor 3 | RUNX3 | 2·49 | 0·19 |

**Table 1.** cont.

| Description | Symbol | Ratio | SD |
|---|---|---|---|
| Spectrin, beta, non-erythrocytic 1 | SPTBN1 | 2·38 | 0·10 |
| BLR1, GTP-binding protein [chemokine (C–X–C motif) receptor 5] | BLR1 | 2·37 | 0·23 |
| Rho GTPase-activating protein 10 | ARHGAP10 | 2·37 | 0·37 |
| Peter pan homologue | PPAN | 2·34 | 0·26 |
| CXXC finger 5 | CXXC5 | 2·33 | 0·15 |
| Pim-1 proto-oncogene | PIM1 | 2·30 | 0·17 |
| CD69 antigen (p60, early T-cell activation antigen) | CD69 | 2·30 | 0·30 |
| Origin recognition complex, subunit 6 homologue-like | ORC6L | 2·23 | 0·14 |
| Prostaglandin E receptor 4 (subtype EP4) | PTGER4 | 2·21 | 0·13 |
| BMP and activin membrane-bound inhibitor homologue | BAMBI | 2·18 | 0·13 |
| Fc receptor-like 4 | FCRL4 | 2·13 | 0·11 |
| Chemokine (C–C motif) ligand 23 | CCL23 | 2·13 | 0·19 |
| Interleukin 4-induced 1 | IL4I1 | 2·12 | 0·04 |

and functional characterization of some of the additional target genes shown in Table 1 will be published separately. In addition to the induction of PIK3R1 that we reported previously, the BCAP (PIK3AP1) RNA is also induced by EBNA-2 (Table 1). BCAP is a tyrosine kinase substrate that connects the B-cell receptor to PI3K activation via the SH2 domains that are present in all of the PIK3R1 regulatory subunits (Okada *et al.*, 2000). Bearing in mind our previous results on PIK3R1 (Spender *et al.*, 2002), its prominent position in the complete-genome list suggested further investigation of this target.

## EBNA-2 induces p55α without the need for intermediate protein synthesis

In our previous study of p85α regulation by EBNA-2 in EREB2.5 cells (Spender *et al.*, 2002), the microarray probe used to detect p85α RNA induction was in the 3′ end of the gene, but the epitope of the antibody used to detect p85α protein was in the N terminus of the protein, marked as AB6 in Fig. 1(a). Western blotting with a different pan-p85α antibody that recognizes epitopes present in p85α, p55α and p50α revealed that it is p55α that is induced by EBNA-2, not p85α (Fig. 1b). The timing of expression of p55α in response to reactivation of EBNA-2 was similar to the timing of expression of LMP-1, which is known to be a direct target of EBNA-2 regulation (Spender *et al.*, 2002). The protein induced in response to EBNA-2 activation was confirmed to be p55α, as it was detected (Fig. 1c) by an antibody specific for the unique N terminus of p55α. The protein also co-migrated on SDS-PAGE with *in vitro*-translated p55α protein expressed from an authentic p55α cDNA (Fig. 1d). The induction of p55α was a consequence of EBNA-2 expression and not an artefact of adding oestrogen to the cells, as EREB2.5 cells in which the ER–EBNA-2 fusion gene was replaced with wild-type EBNA-2 expressed p55α constitutively in the absence of oestrogen (Fig. 1e). An RPA specific for the unique 5′ exon of p55α (Fig. 2a) showed that induction of the mRNA could be detected as early as 2 h after addition of oestrogen to reactivate EBNA-2 (Fig. 2b).

The p55α RNA induction was not prevented by protein-synthesis inhibitors (Fig. 2b), confirming that the p55α promoter is regulated by ER–EBNA-2 without the need for

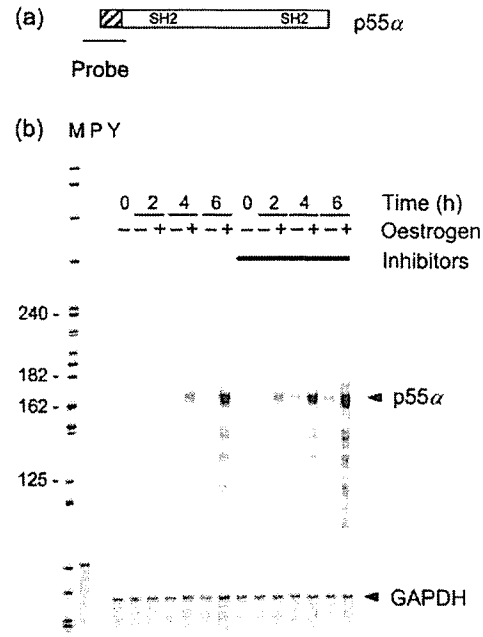


**Fig. 2.** (a) Position of the probe used in the p55α-specific RNase-protection assay (RPA); the unique first exon of p55α is hatched. (b) Regulation of p55α RNA by EBNA-2 in EBV-infected cells. β-Oestradiol-starved EREB2.5 cells were pre-treated for 2 h with protein-synthesis inhibitors or with solvent control and were then either left untreated (–) or were activated by addition of β-oestradiol to the medium (+) for the times indicated. Total cell RNA (10 or 1 μg) was assayed by RPA for p55α or glyceraldehyde-3-phosphate dehydrogenase (GAPDH), respectively. A 164–168 nt protected fragment was produced by the p55α RNA.

any intermediate protein expression. The RPA probe spanned the transcription start site and the length of the protected fragment (164–168 nt) was consistent with initiation of transcription as in the RefSeq cDNA of p55α (GenBank accession no. BC030815).

### p55α is complexed with catalytic subunits in EREB2.5 cells

The system was characterized further by testing expression of the other class I PI3K proteins. As expected, EREB2.5 lymphoid cells expressed all class IA catalytic subunits (Fig. 3a). Regulation of EBNA-2 activity in the EREB2.5 cells by oestrogen had no substantial effect on the protein-expression levels of any of the catalytic subunits (Fig. 3a). For the regulatory subunits, modulation of EBNA-2 activity with oestrogen did not affect the level of p85β or p55γ substantially (Fig. 3b). p85α was generally unaffected by modulation of EBNA-2 activity although, in some experiments, there was a slight reduction upon induction of p55α. No antibody monospecific for p50α is available (the unique first exon only encodes 6 aa), so this could not be tested directly. Several other LCLs were found to express p55α (Fig. 3c), but not all LCLs have it. We have not yet identified the additional factors that may determine whether p55α is induced by EBNA-2 in LCLs.

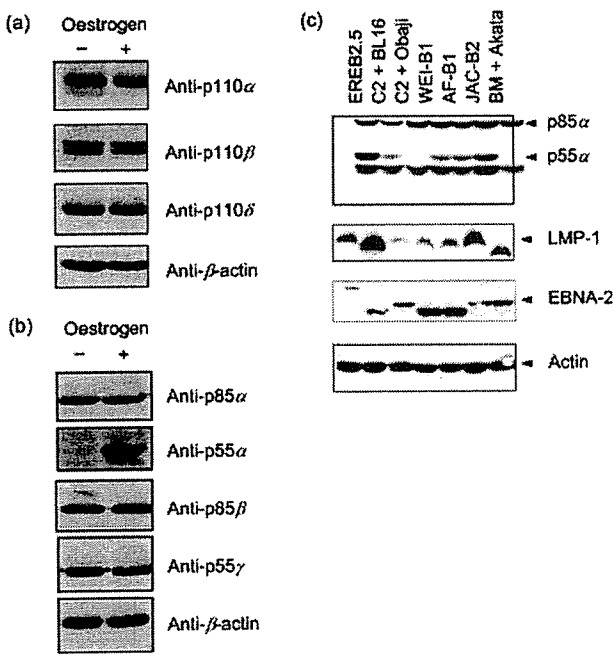


**Fig. 3.** Western blot analysis of PI3K subunits in lysates of oestrogen-starved (−) and β-oestradiol-supplemented (+) EREB2.5 cells. (a) Catalytic subunits. (b) Regulatory subunits. (c) LCLs derived by EBV infection of B cells were analysed by SDS-PAGE and Western blotting for expression of regulatory subunits using the pan-p85α antibody. The samples were also blotted for EBNA-2 and LMP-1 expression and actin as a loading control. EREB2.5, C2+Obaji and C2+BL16 derive from cord B cells; the other LCLs shown are from adult peripheral B cells. C2+BL16, WEI-B1 and AF-B1 have EBV with B type EBNA-2; the other lines have A type EBNA-2.

To test whether the p55α expressed in EREB2.5 cells was complexed with catalytic subunits, p55α was immunoprecipitated from EREB2.5 cell extract and the precipitate was immunoblotted for p110α and p110δ. Both types of catalytic subunit were bound to the p55α induced in the EREB2.5 cells treated with oestrogen (Fig. 4a). The reciprocal immunoprecipitation experiment, with an antibody to p110δ followed by Western blotting to detect all variants of the PIK3R1 regulatory subunit, showed that both p55 and p85 bound to p110δ (Fig. 4b). There were similar proportions of p55α and p85α in the complex; in fact, there was slightly more p55α.

### p55α is required to prevent apoptosis in EREB2.5 cells

Although p55α is not expressed in all LCLs, depletion of p55α in EREB2.5 cells by an RNAi plasmid (Fig. 5a) expressing a sequence from the unique first exon of p55α greatly reduced the proliferation of the cells over a 12 day period (Fig. 5b), indicating that p55α is required for optimal growth or survival of these cells. Two different assays for apoptosis, production of cleaved PARP (Fig. 5c) and accumulation of sub-G1 DNA content in flow cytometry of propidium iodide-stained cell nuclei (Fig. 5d), were used. Both showed a substantial increase in the amount of apoptotic cells in response to p55α RNAi, indicating that p55α plays a significant role in the survival of these cells. By 12 days of p55α RNAi, 35 % of the cells had a sub-G1 DNA content (gate M1, Fig. 5d). Inactivation of EBNA-2 by withdrawal of oestrogen initially caused an arrest of the cell cycle in both G1 and G2 (Kempkes *et al.*, 1995), but then progressive accumulation of cells with a sub-G1 DNA content over this longer time course (Fig. 5d).

## DISCUSSION

A recent report on EBNA-2-regulated RNAs in LCLs (Zhao *et al.*, 2006) used a conditionally functional EBNA-2 allele similar to that used in this study, but did not distinguish direct targets of EBNA2 from genes that might be regulated downstream of the direct EBNA-2 target genes. In our array analysis of EBNA-2 target genes (Table 1), we have used a strategy involving protein-synthesis inhibitors to identify functionally direct targets. It remains to be determined whether these genes are all regulated by EBNA-2 acting as a transcription factor at their promoters, but our strategy provides a set of genes that is likely to include the direct targets of EBNA-2 transcriptional regulation. Some of the newly identified target genes have clear connections with known functions of EBNA-2, for example, in the Notch signalling pathway (HES1 and DTX1).

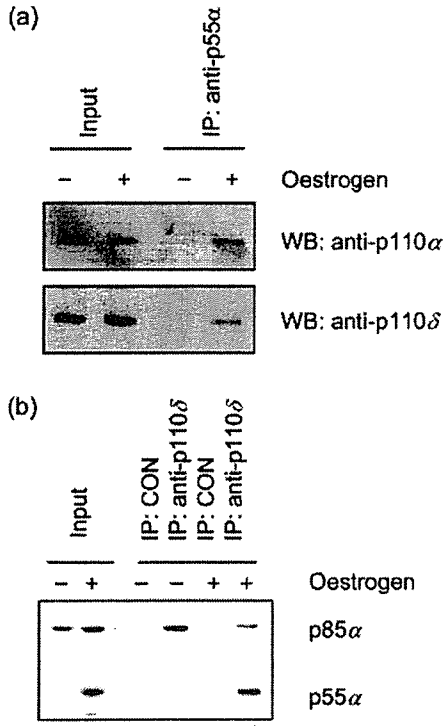


**Fig. 4.** Complexes of catalytic and regulatory subunits of PI3K in EREB2.5 cell extracts. (a) Immunoprecipitation of p55α followed by Western blot for catalytic subunits p110α and p110δ. (b) Immunoprecipitation with anti-p110δ antibodies or control rabbit IgG, followed by Western blot with pan-p85α antibody. Ten per cent of the input amount of protein was also loaded.

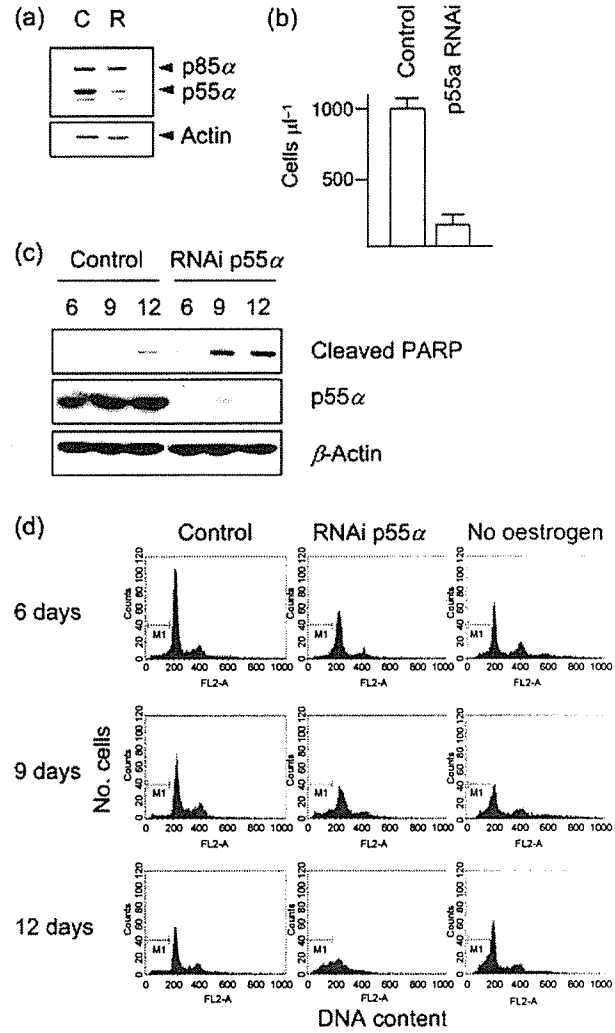


**Fig. 5.** (a) Western blot showing specific reduction of p55α protein levels after transfection with p55α RNAi (R) vector or control (C) vector. (b) Live cell number 12 days after transfection of siRNA vector [cells (μl culture)$^{-1}$]. (c) Protein extracts analysed by Western blotting with antibodies specific for cleaved PARP (Asp 214), p55α or β-actin. (d) Flow-cytometry analysis of propidium iodide-stained cells for DNA content. The M1 gate marks the population of cells with a sub-G1 DNA content. Cells transfected with the p55a RNAi plasmid or the empty vector (control) were analysed after 6, 9 or 12 days selection in hygromycin. The profiles are compared with 6, 9 or 12 days oestrogen withdrawal (no oestrogen). M1 gate values at 12 days were 10, 35 and 23% respectively for control, RNAi p55α and no oestrogen samples.

In this paper, we focus on the PIK3R1 regulation and show that the p55α regulatory subunit of PI3K is induced by EBNA-2 in EREB2.5 lymphoblastoid cells at the RNA level, resulting in expression of the p55α protein. The overlap of the 3′ end of the p55α mRNA with p85α mRNA accounts for the previous data that had been interpreted as an induction of p85α RNA (Spender *et al.*, 2002). The p55α forms complexes with p110 catalytic subunits of PI3K, including p110α and p110δ. Although there are mechanisms by which oestrogen can activate PI3K signalling from membrane ER (Castoria *et al.*, 2001; Tsai *et al.*, 2001) that could potentially complicate the use of an ER–EBNA-2 fusion protein, our experiments show that the induction of p55α in this cell system was clearly mediated by EBNA-2.

Specific depletion of p55α by RNAi in EREB2.5 cells caused apoptosis, indicating that p55α plays a role in maintaining cell survival in this LCL. Several other LCLs also expressed p55α, but some did not, for example C2+Obaji and BM+Akata (Fig. 3c). There was no simple correlation between p55α expression and A or B type EBNA-2 or cord/adult-derived B cells (these details of the cell lines are given in the legend to Fig. 3), so further investigation will be required to understand why only some LCLs have p55α. The variation in size of EBNA-2 and LMP1 in the cell lines is a consequence of variation in copy numbers of repeat sequences in these proteins and is a normal feature of the different virus strains represented.

The specific induction of p55α by EBNA-2 in EREB2.5 cells, with p85α present constitutively, makes it particularly interesting to consider what effects on the cell may be mediated uniquely by p55α. The unique N terminus of p85α contains the bcr region, which binds to cdc42H, a small G protein of the Rho family. Signalling from cdc42H has major effects on the cytoskeleton and cell polarity (Raftopoulou & Hall, 2004; Wilkinson *et al.*, 2005), so this is presumably avoided in signal transduction via p55α. The SH3 domain in the N terminus of p85α is also able to bind to dynamin (Gout *et al.*, 1993). In contrast, the unique N terminus of p55α has been reported to bind to β-tubulin (Inukai *et al.*, 2000), perhaps allowing localization of the activation of downstream signalling to a particular site in the cell. In previous work, overexpression of the individual isoforms and analysis of association with various tyrosine kinase receptors showed some differences and revealed that p55α can be phosphorylated on tyrosine (Inukai *et al.*, 2001). Several studies have examined the role of p50 and p55 in insulin signalling (Inukai *et al.*, 1997; Terauchi *et al.*, 1999), but these point more to a specific function for p50α than p55α. Knockout of all three PIK3R1 regulatory subunits showed a clear role in B-cell survival, an increased proportion of pro-B cells in the bone marrow and a reduced B-cell proliferative response to lipopolysaccharide, but a normal response to interleukin-4 and CD40-L. These effects were, however, not ascribed to any individual regulatory subunit (Fruman *et al.*, 1999a, b). Expression of individual regulatory subunits by transfection into differentiated myotube cells and measurement of PI3K activity in the context of insulin signalling indicated that p85α, p55α and p50α all inhibited PI3K activity (Ueki *et al.*, 2000), but the level of expression of p85α was found to be the important determinant of the resulting signal transduction, partial reduction of p85α levels favouring cell survival but complete depletion causing cell death (Ueki *et al.*, 2002). An increase in the level of p55α RNA and protein has also been reported in response to injury of motor nerves in mice, suggesting a role for PI3K containing p55α in the process of nerve regeneration (Okamoto *et al.*, 2004). Our observation that p55α is induced specifically in human B-cell lines by normal levels of EBNA-2 will thus provide an important opportunity to investigate the physiological significance of p55α in human B cells.

## ACKNOWLEDGEMENTS

We thank Bettina Kempkes, Victor Levitsky and Alan Rickinson for some of the cell lines used in this study, Lesley Regan for access to cord-blood donors and Richard Longnecker for the LMP-2A antibody. Part of the work was supported by the Ludwig Institute for Cancer Research and by the Sixth Research Framework Programme of the European Union, Project INCA (LSHC-CT-2005-018704).

## REFERENCES

**Ali, K., Bilancio, A., Thomas, M. & 14 other authors (2004).** Essential role for the p110δ phosphoinositide 3-kinase in the allergic response. *Nature* **431**, 1007–1011.

**Brennan, P., Mehl, A. M., Jones, M. & Rowe, M. (2002).** Phosphatidylinositol 3-kinase is essential for the proliferation of lymphoblastoid cells. *Oncogene* **21**, 1263–1271.

**Castoria, G., Migliaccio, A., Bilancio, A. & 7 other authors (2001).** PI3-kinase in concert with Src promotes the S-phase entry of oestradiol-stimulated MCF-7 cells. *EMBO J* **20**, 6050–6059.

**Dawson, C. W., Tramountanis, G., Eliopoulos, A. G. & Young, L. S. (2003).** Epstein-Barr virus latent membrane protein 1 (LMP1) activates the phosphatidylinositol 3-kinase/Akt pathway to promote cell survival and induce actin filament remodeling. *J Biol Chem* **278**, 3694–3704.

**End, P., Gout, I., Fry, M. J., Panayotou, G., Dhand, R., Yonezawa, K., Kasuga, M. & Waterfield, M. D. (1993).** A biosensor approach to probe the structure and function of the p85α subunit of the phosphatidylinositol 3-kinase complex. *J Biol Chem* **268**, 10066–10075.

**Fruman, D. A., Snapper, S. B., Yballe, C. M., Alt, F. W. & Cantley, L. C. (1999a).** Phosphoinositide 3-kinase knockout mice: role of p85alpha in B cell development and proliferation. *Biochem Soc Trans* **27**, 624–629.

**Fruman, D. A., Snapper, S. B., Yballe, C. M., Davidson, L., Yu, J. Y., Alt, F. W. & Cantley, L. C. (1999b).** Impaired B cell development and proliferation in absence of phosphoinositide 3-kinase p85α. *Science* **283**, 393–397.

**Fukuda, M. & Longnecker, R. (2004).** Latent membrane protein 2A inhibits transforming growth factor-β1-induced apoptosis through the phosphatidylinositol 3-kinase/Akt pathway. *J Virol* **78**, 1697–1705.

**Gout, I., Dhand, R., Hiles, I. D. & 9 other authors (1993).** The GTPase dynamin binds to and is activated by a subset of SH3 domains. *Cell* **75**, 25–36.

**Inukai, K., Anai, M., Van Breda, E. & 9 other authors (1996).** A novel 55-kDa regulatory subunit for phosphatidylinositol 3-kinase structurally similar to p55PIK is generated by alternative splicing of the p85α gene. *J Biol Chem* **271**, 5317–5320.

**Inukai, K., Funaki, M., Ogihara, T. & 12 other authors (1997).** p85α gene generates three isoforms of regulatory subunit for phosphatidylinositol 3-kinase (PI 3-kinase), p50α, p55α, and p85α, with different PI 3-kinase activity elevating responses to insulin. *J Biol Chem* **272**, 7873–7882.

**Inukai, K., Funaki, M., Nawano, M. & 10 other authors (2000).** The N-terminal 34 residues of the 55 kDa regulatory subunits of phosphoinositide 3-kinase interact with tubulin. *Biochem J* **346**, 483–489.

**Inukai, K., Funaki, M., Anai, M. & 11 other authors (2001).** Five isoforms of the phosphatidylinositol 3-kinase regulatory subunit exhibit different associations with receptor tyrosine kinases and their tyrosine phosphorylations. *FEBS Lett* **490**, 32–38.

**Kaiser, C., Laux, G., Eick, D., Jochner, N., Bornkamm, G. W. & Kempkes, B. (1999).** The proto-oncogene c-*myc* is a direct target gene of Epstein-Barr virus nuclear antigen 2. *J Virol* **73**, 4481–4484.

**Kempkes, B., Spitkovsky, D., Jansen-Durr, P., Ellwart, J. W., Kremmer, E., Delecluse, H. J., Rottenberger, C., Bornkamm, G. W. & Hammerschmidt, W. (1995).** B-cell proliferation and induction of early $G_1$-regulating proteins by Epstein–Barr virus mutants conditional for EBNA2. *EMBO J* **14**, 88–96.

**Kieff, E. & Rickinson, A. B. (2001).** Epstein-Barr virus and its replication. In *Fields Virology*, 4th edn, pp. 2511–2573. Edited by D. M. Knipe & P. M. Howley. Philadelphia, PA: Lippincott Williams & Wilkins.

**Mann, K. P., Staunton, D. & Thorley-Lawson, D. A. (1985).** Epstein-Barr virus-encoded protein found in plasma membrane in transformed cells. *J Virol* **55**, 710–720.

**Okada, T., Maeda, A., Iwamatsu, A., Gotoh, K. & Kurosaki, T. (2000).** BCAP: the tyrosine kinase substrate that connects B cell receptor to phosphoinositide 3-kinase activation. *Immunity* **13**, 817–827.

**Okamoto, T., Namikawa, K., Asano, T., Takaoka, K. & Kiyama, H. (2004).** Differential regulation of the regulatory subunits for phosphatidylinositol 3-kinase in response to motor nerve injury. *Brain Res Mol Brain Res* **131**, 119–125.

**Okkenhaug, K. & Vanhaesebroeck, B. (2003).** PI3K in lymphocyte development, differentiation and activation. *Nat Rev Immunol* **3**, 317–330.

**Portis, T. & Longnecker, R. (2004).** Epstein–Barr virus (EBV) LMP2A mediates B-lymphocyte survival through constitutive activation of the Ras/PI3K/Akt pathway. *Oncogene* **23**, 8619–8628.

**Raftopoulou, M. & Hall, A. (2004).** Cell migration: Rho GTPases lead the way. *Dev Biol* **265**, 23–32.

**Scholle, F., Bendt, K. M. & Raab-Traub, N. (2000).** Epstein-Barr virus LMP2A transforms epithelial cells, inhibits cell differentiation, and activates Akt. *J Virol* **74**, 10681–10689.

**Sinclair, A. J. & Farrell, P. J. (1995).** Host cell requirements for efficient infection of quiescent primary B lymphocytes by Epstein-Barr virus. *J Virol* **69**, 5461–5468.

**Spender, L. C., Cornish, G. H., Sullivan, A. & Farrell, P. J. (2002).** Expression of transcription factor AML-2 (RUNX3, CBFα-3) is induced by Epstein-Barr virus EBNA-2 and correlates with the B-cell activation phenotype. *J Virol* **76**, 4919–4927.

**Spender, L. C., Whiteman, H. J., Karstegl, C. E. & Farrell, P. J. (2005).** Transcriptional cross-regulation of RUNX1 by RUNX3 in human B cells. *Oncogene* **24**, 1873–1881.

**Swart, R., Ruf, I. K., Sample, J. & Longnecker, R. (2000).** Latent membrane protein 2A-mediated effects on the phosphatidylinositol 3-kinase/Akt pathway. *J Virol* **74**, 10838–10845.

**Terauchi, Y., Tsuji, Y., Satoh, S. & 30 other authors (1999).** Increased insulin sensitivity and hypoglycaemia in mice lacking the p85α subunit of phosphoinositide 3-kinase. *Nat Genet* **21**, 230–235.

**Tsai, E.-M., Wang, S.-C., Lee, J.-N. & Hung, M.-C. (2001).** Akt activation by estrogen in estrogen receptor-negative breast cancer cells. *Cancer Res* **61**, 8390–8392.

**Ueki, K., Algenstaedt, P., Mauvais-Jarvis, F. & Kahn, C. R. (2000).** Positive and negative regulation of phosphoinositide 3-kinase-dependent signaling pathways by three different gene products of the p85α regulatory subunit. *Mol Cell Biol* **20**, 8035–8046.

**Ueki, K., Fruman, D. A., Brachmann, S. M., Tseng, Y.-H., Cantley, L. C. & Kahn, C. R. (2002).** Molecular balance between the regulatory and catalytic subunits of phosphoinositide 3-kinase regulates cell signaling and survival. *Mol Cell Biol* **22**, 965–977.

**Wilkinson, S., Paterson, H. F. & Marshall, C. J. (2005).** Cdc42–MRCK and Rho–ROCK signalling cooperate in myosin phosphorylation and cell invasion. *Nat Cell Biol* **7**, 255–261.

**Zhao, B., Maruo, S., Cooper, A., Chase, M. R., Johannsen, E., Kieff, E. & Cahir-McFarland, E. (2006).** RNAs induced by Epstein–Barr virus nuclear antigen 2 in lymphoblastoid cell lines. *Proc Natl Acad Sci U S A* **103**, 1900–1905.

# Divergent regulation of hepatic glucose and lipid metabolism by phosphoinositide 3-kinase via Akt and PKCλ/ζ

Cullen M. Taniguchi,[1] Tatsuya Kondo,[2] Mini Sajan,[3] Ji Luo,[4,5] Roderick Bronson,[6] Tomoichiro Asano,[7] Robert Farese,[3] Lewis C. Cantley,[4,5] and C. Ronald Kahn[1,*]

[1] Cellular and Molecular Physiology, Joslin Diabetes Center, Harvard Medical School, Boston, Massachusetts, 02215
[2] Department of Metabolic Medicine, Graduate School of Medical Sciences, Kumamoto University, Kumamoto, Japan
[3] University of South Florida, College of Medicine, Tampa, Florida 33612
[4] Department of Systems Biology, Harvard Medical School, Boston, Massachusetts, 02215
[5] Division of Signal Transduction, Beth Israel Deaconess Medical Center, Boston, Massachusetts 02115
[6] Department of Pathology, Harvard Medical School, Boston, Massachusetts, 02215
[7] Third Department of Internal Medicine, Faculty of Medicine, University of Tokyo, Tokyo 113, Japan
*Correspondence: c.ronald.kahn@joslin.harvard.edu

## Summary

**Although the class $I_A$ phosphoinositide 3-kinase (PI3K) pathway is central to the metabolic actions of insulin, its mechanism of action is not well understood. To identify the role of the PI3K pathway in insulin regulation of hepatic function, we ablated the expression of both major regulatory subunits of PI3K by crossing mice lacking *Pik3r1* in liver with *Pik3r2* null mice, creating liver-specific double knockout mice (L-p85DKO). L-p85DKO mice failed to activate PI3K or generate $PIP_3$ upon insulin stimulation or activate its two major effectors, Akt and PKCλ/ξ. Decreased Akt activation resulted in increased gluconeogenic gene expression, impaired glucose tolerance, and hyperinsulinemia, while the defective activation of PKCλ/ξ by insulin was associated with hypolipidemia and decreased transcription of SREBP-1c. These data indicate that the PI3K pathway is critical for insulin's actions in the liver in vivo, and that differential regulation by Akt and PKCλ/ξ differentially defines specific actions of insulin and PI3K on hepatic glucose and lipid metabolism.**

## Introduction

Class $I_A$ phosphoinositide 3-kinase (PI3K) is a critical mediator of insulin action in the liver (Taniguchi et al., 2006). Following insulin stimulation of its receptor, PI3K generates the second messenger phosphatidylinositol(3,4,5)-trisphosphate ($PIP_3$), which then activates several downstream targets such as Akt and atypical forms of protein kinase C (PKC λ/ζ) via their colocalization with PDK1. The PI3K-dependent activation of Akt defines many aspects of the insulin-mediated regulation of hepatic glucose metabolism. Akt suppresses gluconeogenesis and activates glycogen synthesis via its phosphorylation of FoxO1 (Zhang et al., 2002) and GSK3β (Cross et al., 1995), respectively. The PI3K/Akt axis also regulates cell growth via the phosphorylation and inhibition of hamartin and tuberin (TSC1 and TSC2) (Potter et al., 2002), which effectively activates the mTOR pathway resulting in phosphorylation of p70S6kinase and 4EBP1and stimulation of protein synthesis and cell growth (Harris and Lawrence, 2003).

Insulin also promotes hepatic lipogenesis through several mechanisms, the most prominent of which is upregulation of sterol regulatory element binding protein-1c (SREBP-1c), a transcription factor that potently activates the lipogenic program (Shimomura et al., 1999). The components of the PI3K pathway that are responsible for this increase in SREBP-1c expression are not well understood. Indeed, while Akt has potent effects on glucose metabolism, it exhibits only modest effects on lipogenesis and SREBP-1c mRNA levels both in vitro (Fleischmann and Iynedjian, 2000) and in vivo (Ono et al., 2003). Moreover, much of Akt's lipogenic effect may occur independently of SREBP (Ono et al., 2003). Recently, the atypical PKC isoforms λ and ζ that are activated by PI3K have been shown to be required for insulin-dependent increases in the expression of SREBP-1c (Farese et al., 2005). Thus, a liver-specific knockout of PKCλ leads to a marked decrease in SREBP-1c expression, with little effect on the expression of gluconeogenic genes, such as phosphoenolpyruvate carboxykinase (PEPCK) and glucose 6-phosphatase (G6Pase), suggesting that the atypical PKCs may positively regulate SREBP-1c expression in vivo (Matsumoto et al., 2003).

The dissection of the multiple functions of PI3K in vivo by genetic deletion has been difficult to achieve. Mammalian PI3K is a heterodimer that consists of an SH2-containing regulatory subunit (p85) and a catalytic subunit (p110), with both subunits expressed in multiple isoforms. There are eight isoforms of the regulatory subunit encoded by three different genes, *Pik3r1*, *Pik3r2*, and *Pik3r3*. In most cells, the gene products of *Pik3r1* constitute 65%–75% of the intracellular pool of regulatory subunits in the form of p85α and its two shorter isoforms p55α and p50α (Ueki et al., 2000), while *Pik3r2* accounts for 20%–30% of the regulatory subunits in the form of p85β (Ueki et al., 2003). The catalytic subunit of class $I_A$ PI3K is also represented by three different isoforms—p110α, p110β, and p110δ—each of which is produced from a distinct gene (reviewed in Shepherd et al., 1998).

The complex roles of the PI3K subunits in embryonic development and metabolic homeostasis have confounded conventional

knockout studies of both the regulatory and catalytic subunits of PI3K. For instance, global knockouts of the p110α or p110β catalytic subunits cause early embryonic lethality (Bi et al., 2002; Bi et al., 1999), and the whole-body knockout of *Pik3r1* results in perinatal lethality (Fruman et al., 2000).

To study the effect of the in vivo loss of the PI3K pathway on hepatic glucose and lipid homeostasis and to circumvent the lethality encountered in various global knockouts of PI3K subunits, we have created mice which lack all PI3K regulatory subunits in liver (L-p85DKO) by crossing mice in which the *Pik3r1* gene (producing p85α, p55α, and p50α) is specifically inactivated in the liver (L-αKO mice) with *Pik3r2* knockout mice, which lack the other major p85 isoform, p85β, in all tissues. We find that deletion of both *Pik3r1* and *Pik3r2* in the liver completely ablates PI3K activity and the accumulation of $PIP_3$ resulting in a 90% decrease in Akt and PKCλ/ζ activation. By reconstitution experiments, we show that the loss of Akt activity in the L-p85DKO animals is linked to the defects in glucose homeostasis such as glucose intolerance and increased expression of gluconeogenic genes, while decreased PKCλ/ζ activity is associated with lower mRNA levels of SREBP-1c and hypolipidemia. These data suggest that the insulin/PI3K pathway regulates hepatic glucose and lipid homeostasis via distinct mediators, with Akt playing a more important role in the former and PKCλ/ζ activating the latter.

## Results

### L-p85DKO mice have significant defects in insulin-stimulated $PIP_3$ generation

Mice lacking *Pik3r1* and *Pik3r2* in liver were generated by crossing mice that were both homozygous for a floxed allele of *Pik3r1* (Luo et al., 2005) and heterozygous for the albumin-Cre transgene (Postic and Magnuson, 2000) with mice homozygous for both the *Pik3r1* floxed allele and the *Pik3r2* null allele (Ueki et al., 2002). Thus, these matings produced mice deleted of *Pik3r1* specifically in liver on a global p85β knockout background, i.e., a double knockout of *Pik3r1* and *Pik3r2* in liver (L-p85DKO). This breeding strategy (see Experimental Procedures) also generated four other study groups: *Pik3r1* homozygous floxed controls (FLOX), *Pik3r1* homozygous floxed mice that also lack *Pik3r2* (βKO), as well as mice with *Pik3r1* ablated only in liver either on a wild-type (wt) background (L-αKO) or on a *Pik3r2* heterozygous background (L-αKOβH). Western blotting with a pan-p85 antibody directed against the common C terminus of the regulatory subunits revealed an ~90% decrease of hepatic p85α and p50α expression in mice with a deletion of *Pik3r1* in liver, which is consistent with the amount of protein derived from hepatocytes (Figure 1A and Fruman et al., 2000). Since the pan-p85α antibody only weakly detects p85β and there are no good existing antibodies for p85β Western blotting, we confirmed the deletion of p85β by quantitative RT-PCR. Indeed, mice that were homozygous for a *Pik3r2* null allele exhibited no detectable levels of p85β mRNA after 40 cycles of quantitative RT-PCR, while mice heterozygous for *Pik3r2* displayed a 30% decrease of p85β mRNA (Figure 1B).

The genetic ablation of the regulatory subunits also decreased total hepatic PI3K activity to levels commensurate with p85 expression. Thus, when total PI3K activity was measured from phosphotyrosine (pTyr) immunoprecipitates of liver lysates, βKO animals that lack only 20% of total regulatory subunits exhibited no differences from FLOX controls. More severe disruptions of p85 expression, as in the L-αKO (L-*Pik3r1*$^{-/-}$, *Pik3r2*$^{+/+}$) or the L-αKOβH (L-*Pik3r1*$^{-/-}$, *Pik3r2*$^{+/-}$) mice, caused a 50% and 70% reduction in pTyr-associated PI3K activity, respectively (Figure 1C). As expected, when all four alleles of the regulatory subunits were deleted (L-*Pik3r1*$^{-/-}$, *Pik3r2*$^{-/-}$; L-p85DKO), insulin failed to stimulate PI3K activity above basal levels. In general, IRS-1- and IRS-2-associated PI3K activity reflected total PI3K activity, except that the loss of one or both alleles of *Pik3r2* resulted in increased IRS-2 activity, as previously noted (Ueki et al., 2002).

Germline knockouts of the regulatory subunit of PI3K have been complicated by discrepancies between PI3K activity and $PIP_3$ levels due to various compensatory effects (Terauchi et al., 1999). To determine levels of the second messenger $PIP_3$ in these knockout animals, we utilized an in situ immunofluorescence technique that allowed us to semiquantitatively measure $PIP_3$ levels in hepatocytes with an anti-$PIP_3$ antibody (Figure 1D; Kitamura et al., 2004). Surprisingly, $PIP_3$ levels in βKO and L-αKO mice were not statistically different from control FLOX mice, despite a 50% decrease in total PI3K activity in the latter (Figure 1C). More stringent deletions of regulatory subunits did produce statistically significant decreases in $PIP_3$ levels. L-αKOβH mice showed a 50% impairment of $PIP_3$ generation, while insulin-stimulated $PIP_3$ production in L-p85DKO mice was barely above basal levels. Thus, genetic ablation of the major regulatory subunit isoforms encoded by *Pik3r1* and *Pik3r2* can disrupt PI3K activity and function but only after severe deletions of at least three of the four major alleles encoding regulatory subunits.

### Akt signaling is significantly impaired in L-p85DKO mice

The generation of $PIP_3$ by PI3K ultimately activates Akt, atypical PKCs, and other PH domain-containing proteins. As expected, L-p85DKO mice showed a 90% decrease in Akt activation, as measured by phosphorylation of serine 473 in Akt (Figure 2A). This correlated with impaired phosphorylation/activation of downstream Akt targets, including FoxO1 and GSK3β (Figure 2A). The phosphorylation of TSC2 was also significantly impaired (Figure 2B). Since TSC2 controls cell growth and protein synthesis via the mTOR/p70S6K pathway, we determined whether the loss of PI3K activity also disrupted mTOR signaling by measuring S6 phosphorylation since phosphorylation of ribosomal S6 is one of the ultimate downstream results of mTOR activation. As expected, insulin stimulation of S6 ribosomal protein phosphorylation exhibited a marked decrease in liver of L-αKOβH mice and was absent in L-p85DKO mice (Figure 2B).

Recent evidence has demonstrated that the different Akt isoforms may have unique roles in metabolic homeostasis (Jiang et al., 2003), with Akt2 playing a particularly dominant role in hepatic metabolism (Cho et al., 2001). To determine if the Akt isoforms were differentially affected by the deletion of p85, we measured the kinase activity of Akt1 (Figure 2C) and Akt2 (Figure 2D) using isoform-specific antibodies (Sakamoto et al., 2002). The kinase activities of both Akt1 and Akt2 paralleled Ser473 phosphorylation of Akt, with activity remaining normal unless all four alleles of p85 were deleted (Figures 2C and 2D). These data suggest that Akt is exquisitely sensitive to $PIP_3$ levels, and that even with a 50% decrease in $PIP_3$ generation, there is sufficient $PIP_3$ to promote the full activation of all Akt isoforms.

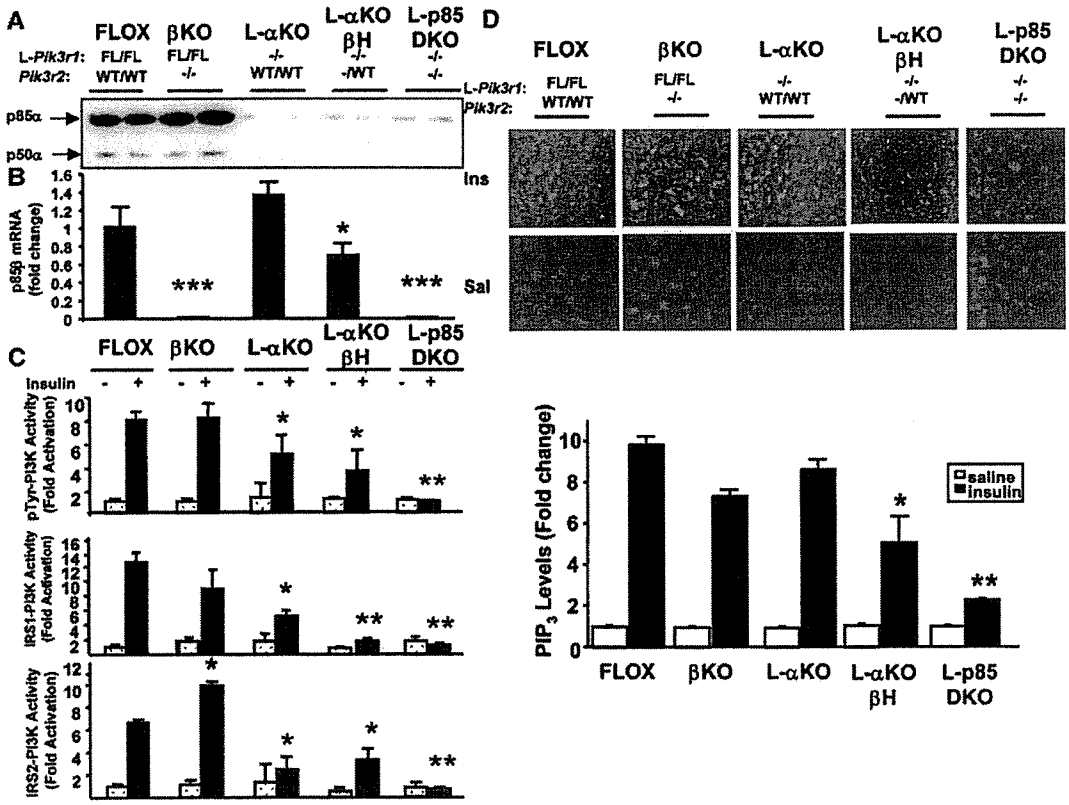


**Figure 1.** L-p85DKO mice have defective insulin-stimulated PI3K activity in liver

**A)** Immunoblot with a pan-p85α from liver lysates of mice of the indicated genotypes.

**B)** Quantitative RT-PCR analysis of p85β message levels. Bars represent means ± SEM, n = 6–8, *p < 0.05 compared to FLOX.

**C)** PI3K activity in pTyr, IRS-1, and IRS-2 immunoprecipitates. Bars represent means ± SEM, n = 4, *p < 0.05 compared to insulin stimulated FLOX.

**D)** (Top) Immunofluorescent staining with a primary anti-$PIP_3$ antibody (IgM) and an anti-mouse secondary antibody conjugated to Alexafluor Red. The sections were counterstained with DAPI. (Bottom) Quantification of the immunofluorescence from $PIP_3$ staining. Four representative slides were chosen from each mouse and the fluorescence intensity of 16 fields per slide was measured and analyzed with VH-H1A5 Analyzer software (KEYENCE, Osaka, Japan). Bars represent means ± SEM, *p < 0.05 compared to insulin-stimulated FLOX. **p < 0.01 and ***p < 0.0001.

## L-p85DKO mice have severe defects in glucose homeostasis

The loss of the insulin stimulated activation of PI3K and Akt in the liver of L-p85DKO mice and led to significant defects in whole-body glucose homeostasis. Compared to FLOX controls, L-p85DKO mice exhibited mild to moderate hyperglycemia in both the fasted and fed states (Figures 3A and 3C). Furthermore, these blood glucose levels occurred in the fast of significant hyperinsulinemia, with insulin levels increased by 4-fold over control animals in L-p85DKO mice in both the fasted and fed states (Figures 3B and 3D). Interestingly, L-αKO mice exhibited improved glucose and insulin levels compared to controls, consistent with previous observations in mice lacking p85α (Fruman et al., 2000; Terauchi et al., 1999).

In addition, L-p85DKO mice exhibited insulin resistance and glucose intolerance. Following an intraperitoneal insulin injection (Figure 3E), mice lacking all hepatic PI3K regulatory subunits in liver showed a significant decrease in insulin sensitivity compared to FLOX controls, as determined by the area under the curve for fall in glucose levels (Figure 3F). Interestingly, L-p85DKO mice exhibit whole-body insulin resistance despite the fact that tissues other than the liver are only homozygous null for p85β, a defect that has previously been shown to improve insulin sensitivity (Ueki et al., 2002). L-p85DKO also exhibited markedly abnormal glucose tolerance tests consistent with diabetes (Figure 3G). For the L-p85DKO mice, the area under the curve was almost three times that of control mice (Figure 3H), whereas L-αKO mice exhibited improved glucose tolerance compared to FLOX controls (Figures 3G and 3H). Thus, while a partial deletion of the regulatory subunits may improve glucose homeostasis, loss of all PI3K regulatory subunits in liver results in diabetes.

## The loss of hepatic PI3K/Akt activity leads to increased gluconeogenesis

One of the hallmarks of diabetes is increased hepatic glucose output due to failure of insulin to inhibit hepatic gluconeogenesis. Since L-p85DKO mice cannot activate Akt and thus phosphorylate and inactivate FoxO1, a key regulator of gluconeogenic gene expression, we posited that the gluconeogenic gene cassette should be dysregulated. Indeed, the mRNA levels of critical regulators of gluconeogenesis: PEPCK (*Pck1*), fructose 1,6-bisphosphatase (*Fbp1*), and glucose-6-phosphatase

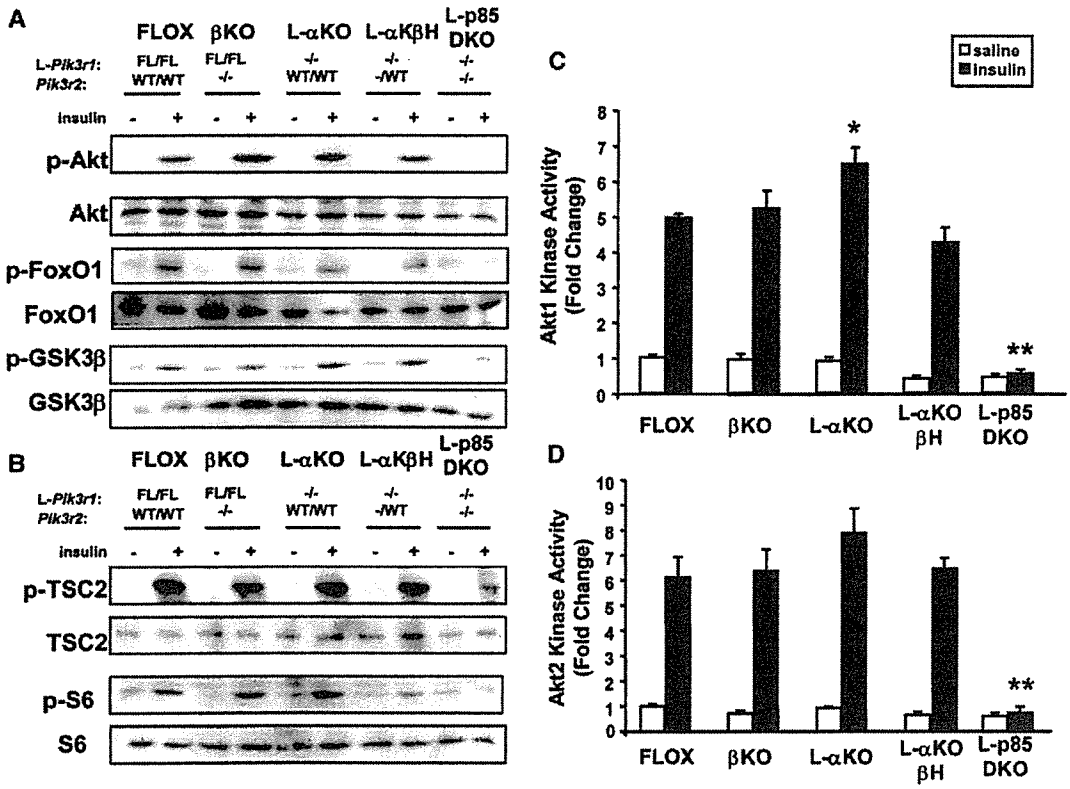


**Figure 2.** Loss of Hepatic PI3K Activity Leads to Defects in the Akt signaling

**A)** Liver lysates from insulin-stimulated mice of the indicated genotype were blotted with antibodies against phospho-Akt (Ser473), phospho-FoxO1 (Ser256), phospho-GSK3β (Ser9). The blots were then stripped and reprobed with antibodies to measure total protein levels.

**B)** Westerns against phospho-TSC2 (Thr1462) and phospho-S6 proteins (Ser240/244). The blots were then stripped and reprobed with antibodies to measure total protein levels. The Western blots in this figure are representative of at least three independent experiments.

**C)** Akt1 and **(D)** Akt2 kinase assays. (Bars represent ± SEM, n = 6, *p < 0.05, **p < 0.001, compared to FLOX + insulin).

(*G6pc*) in the L-p85DKO mice were increased 1.5- to 2.2-fold compared to controls (Figure 4A).

To determine whether this altered pattern of hepatic gene expression resulted in a functional defect, we subjected L-p85DKO mice and littermate FLOX and βKO controls to a pyruvate challenge. In fasting mice, pyruvate is shuttled through the gluconeogenic pathway in the liver and ultimately converted to glucose. Thus, by measuring blood glucose after a peritoneal injection of a pyruvate bolus, we are afforded a physiologic readout of the relative activity of the enzymes of the gluconeogenic pathway. Following an injection of pyruvate, L-p85DKO mice produced significantly more glucose than FLOX and βKO controls (Figure 4B), which indicate that the defects in glucose homeostasis in L-p85DKO mice may stem from the inappropriate gluconeogenesis in the liver due to a failure of insulin to activate PI3K and Akt.

### L-p85DKO mice exhibit altered lipid metabolism

To better understand how the PI3K pathway affects lipid homeostasis, we measured serum levels of triglycerides, cholesterol, and free fatty acids (Figures 5A–5C). L-p85DKO mice showed a 46% reduction in serum triglycerides, a 38% reduction in total serum cholesterol, and a 35% reduction in free fatty acids compared to FLOX controls, which were all statistically significant. The other study groups were not statistically different from controls. These physiologic changes correlated with changes in the molecular machinery that produce hepatic lipids, as the mRNA expression of SREBP-1c (*Srebf1c*) and fatty-acid synthase (*Fasn*) were significantly decreased in L-p85DKO mice (Figure 5D). Interestingly, L-αKOβH mice also showed a statistically significant decrease in *Srebf1c* expression, whereas the other genotypes did not exhibit changes in either of these regulators of lipid metabolism. Since Akt activity was not diminished in these mice, we wondered if other $PIP_3$-dependent kinases, such as PKCλ/ζ, could be responsible for regulating the expression of *Srebf1c*.

Given the prominent role that PKCλ/ζ may play in regulating mRNA levels of SREBP-1c (Matsumoto et al., 2003), we measured PKCλ/ζ kinase activity and found that insulin normally activated PKCλ/ζ in FLOX, βKO, and L-αKO mice (Figure 5E), whereas both L-αKOβH mice and L-p85DKO mice exhibited significant defects in PKCλ/ζ activation, where insulin only marginally activated the kinase above basal levels. The magnitude of PKCλ/ζ activity paralleled the levels of *Srebf1c* expression, as has been noted in other studies (Matsumoto et al., 2003; Standaert et al., 2004).

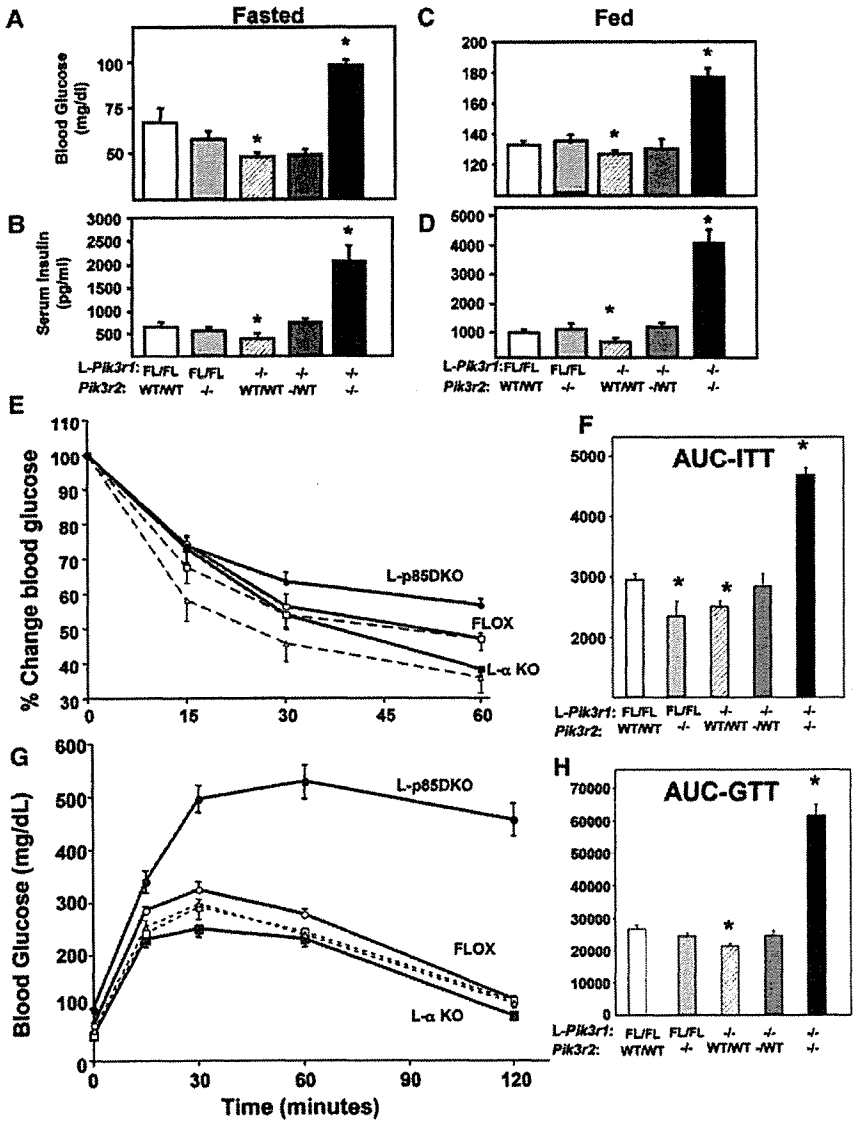


**Figure 3.** L-p85DKO exhibit significant defects in glucose homeostasis

Blood glucose and serum insulin levels in the fasted (**A** and **B**) and random fed (**C** and **D**) states. Glucose and insulin levels are plotted as the mean ± SEM (n = 6–12 mice per genotype).

**E)** Insulin tolerance tests (1 U/kg, intraperitoneally). Results represent blood glucose concentration as a percentage of starting value at zero time and are expressed as means ± SEM (n = 6–8).

**F)** Results from (**E**) expressed as area under ITT curves (see Experimental Procedures).

**G)** Glucose tolerance tests (2 g/kg, intraperitoneally) were performed on mice following a 16 hr fast. Blood samples were collected and glucose measured at the times indicated.

**H)** Results from (**G**) expressed as area under GTT curves (see Experimental Procedures). Bars equal ± SEM, *$p < 0.05$ compared to FLOX.

Open circles (○), bold line—FLOX; open triangles (△), dashed line—βKO; closed squares (■), bold line—L-αKO; open squares (□), dashed line—L-αKOβH; closed circles (●), bold line—L-p85DKO.

### The Activation of PKCλ/ζ, but not Akt, is sufficient to upregulate hepatic SREBP-1c expression

To clarify whether Akt or PKCλ/ζ plays the dominant role in activating SREBP-1c, we reconstituted the livers of L-p85DKO mice with constitutively active forms of Akt (Myr-Akt) or PKCλ (CA-PKCλ) using adenovirus-mediated gene transfer, which specifically targets the liver (Taniguchi et al., 2005). We reasoned that the hepatic expression of constitutively active constructs in fasted L-p85DKO mice would greatly reduce the possibility of surreptitious activation of SREBP-1c by mechanisms unrelated to Akt or PKCλ/ζ. Littermate FLOX and βKO mice were also injected with these adenoviruses as genetic controls.

We first verified that we achieved the proper expression of these constructs in the liver by Western blot and kinase assay. Both constitutively active gene products are distinguishable by Western since the myr-Akt construct contains a C-terminal myc-tag (Sakoda et al., 2003) while the constitutively active PKCλ construct lacks its autoinhibitory pseudosubstrate domain and is thus truncated by approximately 15 kDa compared to wt PKCλ (Kotani et al., 1998). Immunoblots for Akt and PKCλ demonstrated that the tail vein injections successfully expressed the constitutively active constructs in the liver (Figure 6A). These constructs also increased the relative activity of each kinase, where the injection of Myr-Akt adenovirus caused a 6.0- to 8.5-fold increase in total Akt activity (Figure 6B), and the CA-PKCλ virus resulted in a 3.0- to 4.0-fold increase in PKCλ activity compared to fasted FLOX mice treated with control LacZ adenovirus (Figure 6C).

As expected, introduction of the Myr-Akt adenovirus to either the FLOX, βKO, or L-p85DKO mice resulted in the profound inhibition of both *Pck1* and *G6pc* expression in liver in all genotypes, compared to the fasted FLOX control treated with LacZ (Figures 6D and 6E). Interestingly, expression of CA-PKCλ also inhibited the expression of *Pck1* by 65%–75% and *G6Pc* by 50%–60% in all genotypes (Figures 6D and 6E), though only the *Pck1* expression was significantly different from fasted FLOX controls treated with LacZ.

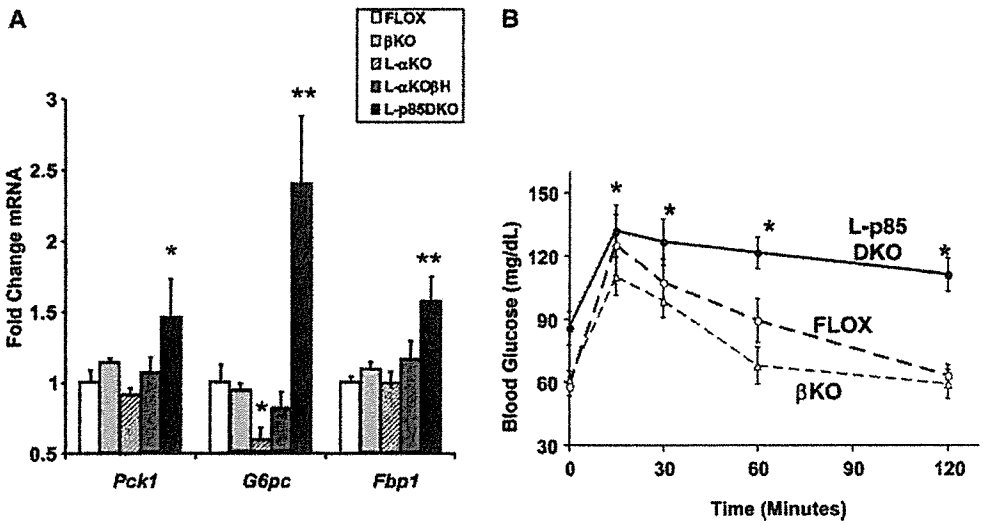


**Figure 4.** Defects in glucose homeostasis are linked to increased gluconeogenesis

**A)** Quantitative RT-PCR analysis of mRNA levels of phosphoenolpyruvate carboxykinase (*Pck1*), glucose-6-phosphatase (*G6Pc*), and fructose-1,6-bisphosphatase (*Fbp1*) in mice of the indicated genotypes.

**B)** Pyruvate challenge of L-p85DKO and control FLOX and βKO mice. Following a 16 hr fast, mice were injected intraperitoneally with a 2 g/kg bolus of pyruvate in normal saline. Blood glucose was then measured at the indicated time points. Open circles (○), bold dashed line—FLOX; open triangles (△), dashed line—βKO; closed circles (•), bold line—L-p85DKO. (Bars equal ± SEM, *$p < 0.05$, **$p < 0.01$ compared to FLOX.)

The expression of SREBP-1c mRNA, on the other hand, was increased by 5- to 6-fold in all genotypes by CA-PKCλ, demonstrating that atypical PKC activity is sufficient to increase *Srebf1c* levels (Figure 6F). Constitutive Akt activity, on the other hand, had no discernable effect on fasting *Srebf1c* expression as compared to mice treated with LacZ. These data demonstrate

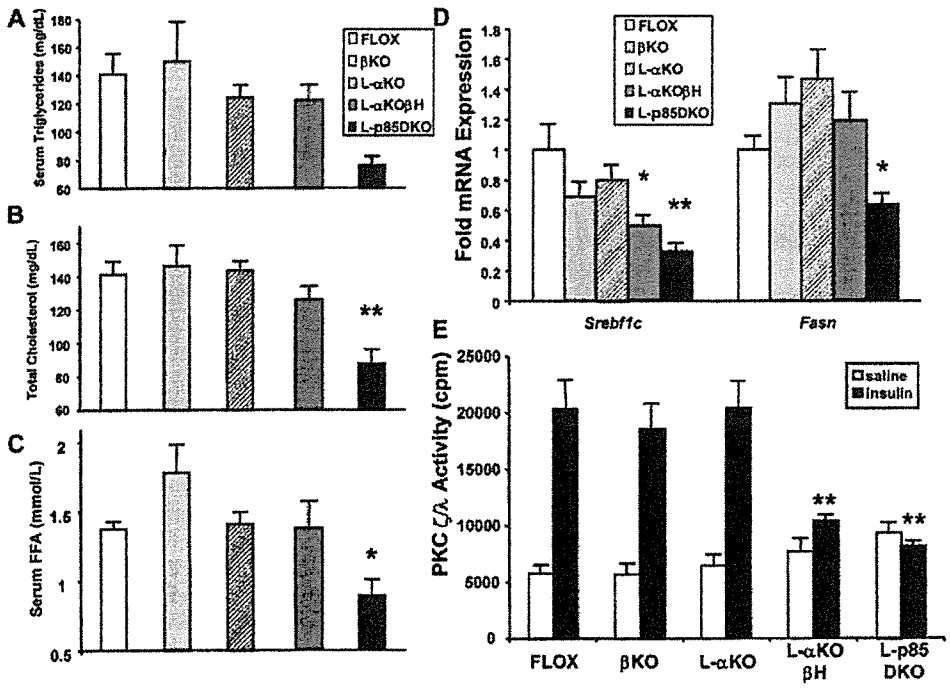


**Figure 5.** L-p85DKO mice are hypolipidemic

**A)** Serum triglycerides **(B)** cholesterol and **(C)** free fatty acids in mice of the indicated genotype (n = 6–8 ± SEM, *$p < 0.05$).

**D)** Quantitative RT-PCR analysis of mRNA levels of SREBP-1c (*Srebf1c*) and fatty-acid synthase (*Fasn*) in mice of the indicated genotypes (n = 6–8 ± SEM *$p < 0.05$, **$p < 0.01$, compared to FLOX).

**E)** Kinase activity of atypical protein kinase C (PKC ζ/λ) expressed as cpm. (n = 3–4 ± SEM, **$p < 0.01$, compared to FLOX + insulin.)

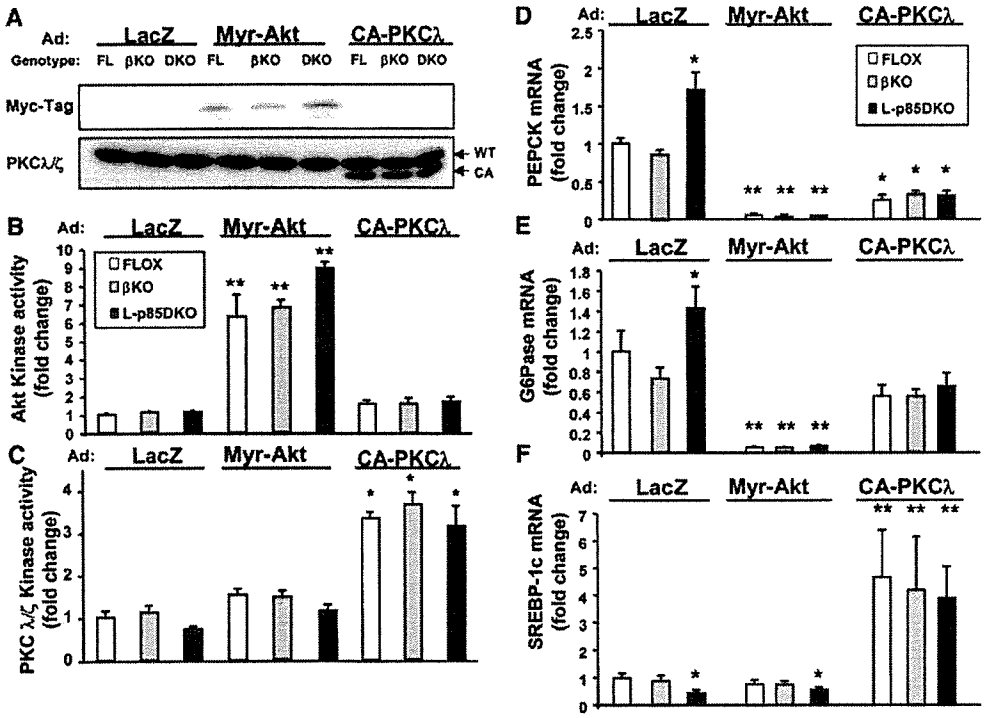


**Figure 6.** PKCλ/ζ activity is sufficient to increase levels of hepatic *Srebf1c* expression

**A)** Western blots against myc-tagged myristoylated Akt and total PKCλ/ζ in liver lysates of mice injected with the indicated adenovirus. The CA-PKCλ construct runs approximately 15 kDa smaller than wt PKCλ because it lacks the autoinhibitory pseudosubstrate domain (~115 amino acids).

**B)** Akt kinase activity and **(C)** PKCλ/ζ kinase activity from liver lysates of fasted mice of indicated genotype and injected with the indicated adenovirus. Quantitative RT-PCR analysis of **(D)** *Pck1*, **(E)** *G6Pc*, and **(F)** *Srebf1c* of fasted mice of indicated genotype, injected with the indicated adenovirus. The error bars represent ± SEM (n = 6–8, *p < 0.05, **p < 0.001, compared to FLOX + LacZ).

that the activity of PKCλ/ζ mediated via the PI3K pathway, and not the activity of Akt, defines the level of insulin effect on SREBP-1c expression.

### Loss of hepatic PI3K causes altered liver growth and compensatory changes in body fat

The PI3K/Akt axis mediates cell growth and protein synthesis through its activation of the mTOR in a pathway involving TSC2 and p70S6 kinase. Since L-p85DKO mice exhibit significant defects in TSC2 phosphorylation and mTOR activation (Figure 2), we posited that L-p85DKO mice may also have defects in hepatocyte growth. Indeed, the livers of L-p85DKO mice were ~40% smaller than the livers of wt mice (Figure 7A). Histological examination of these livers revealed a significant increase in the number of pyknotic cells and scattered lymphocytic infiltrates in four of the five livers analyzed (Figure 7B). The livers of other genotypes were largely normal, though a small percentage of mice lacking *Pik3r1* in liver exhibited a mild degree of hepatic necrosis, as reported earlier (Fruman et al., 2000). Livers lacking all PI3K regulatory subunits were also remarkable for the presence of megahepatocytes that ranged between 40 and 60 microns in diameter as compared to an average normal hepatocyte size of between 15 and 24 microns (Figure 7B). These megahepatocytes were notable for large nuclei with cytoplasmic inclusions, indicating that these cells were likely polyploid with highly abnormal cellular function. Whether these megahepatocytes are formed from abnormal hepatocyte growth or are a product of cell fusion mediated by inflammation is unknown.

This abnormal liver histology correlated with increased levels of the hepatic enzymes, aspartate aminotransferase (AST) and alanine aminotransferase (ALT), and decreased levels of albumin in the serum of L-p85DKO (Table S1). In addition, total bilirubin levels were significantly elevated with no detectable level of direct bilirubin indicating a rise in indirect, or unconjugated, bilirubin. The presence of decreased albumin, increased AST, ALT, indirect bilirubin, and pyknotic cells in the histological samples in L-p85DKO mice is consistent with some destruction of hepatocytes and altered hepatic function (Figure 7B). The other genotypes did not display a significant increase in serum levels of AST, ALT, or bilirubin; a significant decrease in albumin; or any histological changes.

We were somewhat surprised to find that the smaller livers in L-p85DKO mice did not translate to lower overall body weights, as there were no significant weight differences between genotypes, except for a slight increase in total body weight in βKO mice (Figure 7C). We weighed other tissues in the body to determine if the weight of any one particular tissue could account for this difference, of if the normalized weight was due to a general enlargement of other tissues to maintain body weight. Surprisingly, the epididymal fat pads of the L-p85DKO mice were 2-fold heavier than the epididymal fat pads of control FLOX

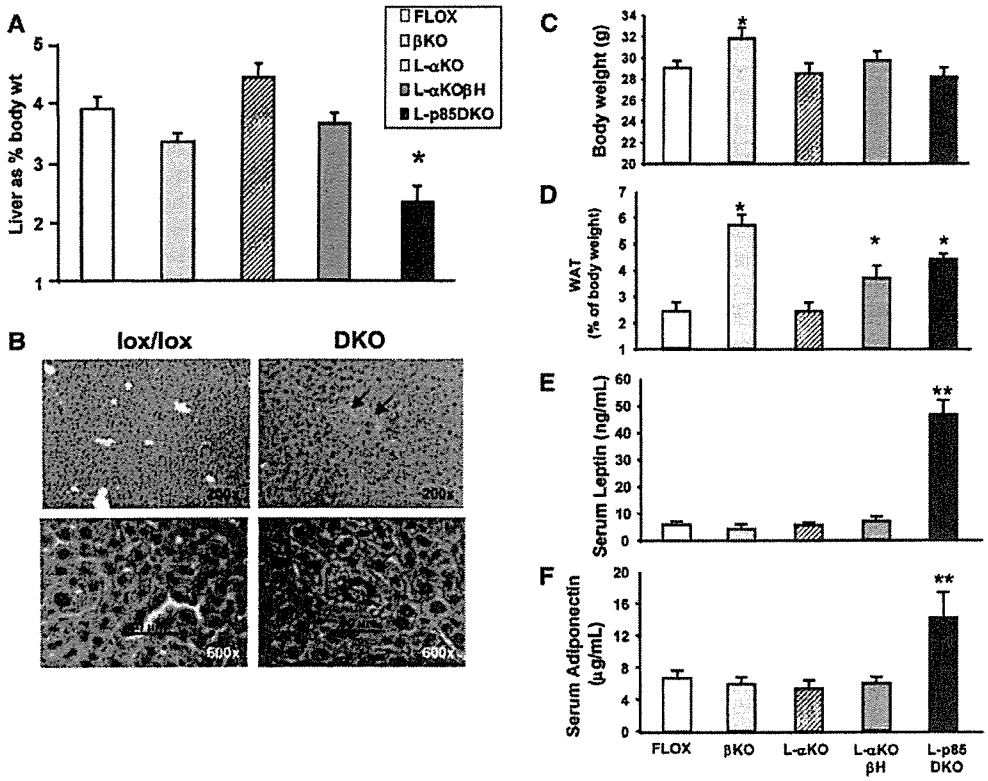


**Figure 7.** Lack of hepatic PI3K activity results in altered liver morphology and adipose tissue size and function

**A)** Liver weights from mice of the indicated genotype, normalized to total body weight.

**B)** Histology of L-p85DKO livers compared to control livers. Note the presence of megahepatocytes (bottom right panel) that are scattered in clusters throughout the field in L-p85DKO livers (indicated by arrows in upper right panel).

**C)** Total body weight and **(D)** epididymal fat pad weights of mice of the indicated genotypes.

**E)** Serum leptin and **(F)** serum adiponectin of various knockout mice. The bars represent ± SEM (n = 6–8, *$p < 0.05$, **$p < 0.01$, compared to FLOX).

mice, while the epididymal fat pads of βKO mice were almost 3-fold larger than controls, and the epididymal fat pads of L-αKOβH mice were ~1.8-fold greater than controls (Figure 7D).

This increase in adipose mass was accompanied by an 8-fold increase in serum leptin levels (Figure 7E) and a 2.5-fold increase in adiponectin levels (Figure 5F) in L-p85DKO mice. There was no change in these circulating adipokines in other genotypes.

## Discussion

Insulin is a powerful anabolic hormone whose function in liver is to suppress gluconeogenesis and activate lipogenesis during times of nutrient excess. Thus, the loss of ablation of insulin action in liver would be predicted to cause unfettered gluconeogenesis, decreased lipogenesis, and diabetes, which is the phenotype observed in L-p85DKO mice. Interestingly, the metabolic defects of L-p85DKO mice are similar to the severe glucose intolerance and hypolipidemia observed in liver insulin receptor knockout (LIRKO) mice, further demonstrating that PI3K mediates most of insulin's regulatory functions in the liver (Michael et al., 2000).

While the prominence of the PI3K pathway in hepatic insulin action has been posited for some time, the molecular mediators of insulin's effect on glucose and lipid metabolism have only recently been explored. Our data agree with several other reports that hepatic glucose metabolism is regulated strongly by PI3K/Akt (Puigserver et al., 2003; Zhang et al., 2002). The loss of PI3K/Akt in the L-p85DKO mice impairs Akt activation by 90% and results in the increased expression of the gluconeogenic genes *Pck1*, *G6Pc*, and *Fbp1*. Conversely, the introduction of a constitutively active Akt into the livers of L-p85DKO or control animals causes >90% reduction of fasting levels of *Pck1* and *G6pc*. We also found that this regulation of gluconeogenesis was not dependent on differences in activity between Akt1 or Akt2. While we cannot rule out the possibility that the various Akt isoforms may interact with different downstream mediators or have different subcellular localization, our data suggest that it is unlikely that the differences in the biology of the Akt isoforms comes from the upstream activation by PI3K since both Akt1 and Akt2 maintained full activation until $PIP_3$ was fully depleted in the L-p85DKO mice.

While Akt has been clearly demonstrated to mediate insulin's suppression of gluconeogenesis, the role of Akt in the regulation of insulin-mediated lipogenesis is more controversial. Our data indicate that Akt may play only a minor role in activating lipogenesis, as the administration of a constitutively active Akt adenovirus to L-p85DKO or control animals failed to increase *Srebpf1c* levels in fasted animals. On the other hand, we demonstrated

that atypical PKC activity alone is sufficient to increase the expression of *Srebf1c* since the expression of a constitutively active PKCλ/ζ construct specifically in the hepatocytes of L-p85DKO or control animals upregulated *Srebf1c* expression 5- to 6-fold over fasted control animals injected with LacZ adenovirus. The converse relation may also be true since L-αKOβH and L-p85DKO both exhibited significant impairments in both PKCλ/ζ activity and *Srebf1c* expression. These data complement and significantly expand upon previously published knockout studies that demonstrate that atypical PKC activity is necessary for insulin-induced *Srebf1c* expression (Matsumoto et al., 2003). Together, these data suggest a primary role of PI3K/atypical PKCs in regulating *Srebf1c* levels in response to insulin.

The precise mechanisms by which PKCλ/ζ increases the transcription of SREBP-1c are not well understood. The liver X receptor (LXR) pathway has been postulated to play a primary role in the insulin-mediated induction of *Srebf1c* message levels (Chen et al., 2004). Whether the atypical PKCs interact with any factor related to the LXR pathway is not known, however, since the in vivo substrates of the atypical PKCs have not yet been defined. Indeed, the elucidation of the targets of PKCλ/ζ will be essential to understanding the molecular basis of aPKC-dependent regulation of SREBP-1c transciption.

Interestingly, the divergence in insulin's regulation of hepatic glucose and lipid was detected due to a difference in the activation of Akt and aPKC in the various p85 hypomorphs. Our data suggest that Akt may be more sensitive to insulin/$PIP_3$ than PKCλ/ζ since Akt could be fully activated in the αKOβHet mice despite the fact the levels of $PIP_3$ were reduced by ~50% (see Figure 1D), while PKCλ/ζ activity in these mice was markedly diminished (see Figure 5E). The molecular basis for this differential activation is not known but could be due to differences in their $PIP_3$ binding or some other aspect of aPKC activation, such as autophosphorylation or inhibition by its pseudosubstrate domain (Farese et al., 2005).

Phosphoinositide 3-kinase controls several other important aspects of hepatocyte function in addition to metabolism. In particular, the PI3K/Akt/mTOR pathway was severely impaired in L-p85DKO mice as manifested by decreased TSC2 and S6 phosphorylation. These defects in translational control by PI3K lead to a 40% decrease in liver size and a 60% decrease in albumin synthesis. In addition, L-p85DKO mice exhibited abnormal histology and elevated levels of serum AST, ALT, and indirect (unconjugated) bilirubin (see Table S1). Despite these indications of liver damage, L-p85DKO mice were able to respond in an exaggerated way to a pyruvate challenge (Figure 4B), indicating that the hyperglycemia and probably the other defects in glucose homeostasis in L-p85DKO mice were a result of the increased expression of functional gluconeogenic enzymes (Figure 4A), and not some aspect of hepatic insufficiency.

The loss of hepatic PI3K activity also led to changes in adipose tissue physiology. The epididymal fat pads in the L-p85DKO were almost 2-fold larger than controls, which is most likely due to the moderate and persistent hyperinsulinemia that leads to a substrate shift to adipocytes. This phenomenon has been observed in other models of insulin resistance and diabetes such as liver insulin receptor knockout (LIRKO) mice (Michael et al., 2000) and muscle insulin receptor knockout (MIRKO) mice (Bruning et al., 1998). In addition, L-p85DKO mice exhibited significant increases in the two major adipokines, leptin and adiponectin. These increases are probably not a cell-autonomous effect of adipose tissue since the elevated leptin and adiponectin are increased only in the L-p85DKO mice, despite the βKO and L-αKOβH mice having epididymal fat pads nearly equal in size or larger than those in the L-p85DKO mice. Interestingly, LIRKO mice also display striking increases in serum leptin levels (>60-fold over controls) as a compensatory response to a 450-fold increase in soluble leptin receptor expression by the liver (Cohen and C.R.K., unpublished data). The relationship between insulin-stimulated PI3K activity and leptin receptor expression observed in LIRKO may also explain the elevated leptin levels in L-p85DKO mice, as L-p85DKO mice have a 12-fold increase in soluble leptin receptor expression (data not shown) to match the 5-fold increase in serum leptin (Figure 7E).

In summary, deletion of all major regulatory subunits of PI3K in liver results in a marked reduction in insulin-stimulated PI3K activity and $PIP_3$ accumulation in liver and significant defects in glucose and lipid homeostasis, as well as in hepatic size and function. Thus, the PI3K pathway is essential for metabolic homeostasis and cell growth, and PI3K activity is responsible for nearly all of insulin's actions in the liver in vivo. Moreover, the specific regulation of glucose and lipid homeostasis by insulin diverges after PI3K activation, where it appears that Akt selectively and potently regulates gluconeogenesis whereas PKCλ/ζ increases *Srebf1c* expression. The differential actions of the PI3K-dependent kinases, Akt and PKCλ/ζ, may represent the primary mechanisms by which insulin regulates different aspects of hepatic metabolism. Understanding these mechanisms not only helps to clarify the important regulators in hepatic function but may also provide more specific ways to improve many complications of diabetes and the metabolic syndrome.

## Experimental procedures

### Animals and breeding strategy

All animals were housed on a 12 hr light-dark cycle and fed a standard rodent chow. All protocols for animal use and euthanasia were approved by the Animal Care Use Committee of the Joslin Diabetes Center and Harvard Medical School in accordance with National Institutes of Health guidelines. All mice in this study were on a 129Sv-C57BL/6-FVB mixed genetic background. The breeding strategy in this study involved the crossing of homozygous floxed *Pik3r1* mice with *Pik3r2* homozygous null mice to create mice homozygous for both the *Pik3r1* floxed allele and the *Pik3r2* null allele (*Pik3r1*$^{fl/fl}$, *Pik3r2*$^{-/-}$). These mice were then bred with L-αKOβH (L-*Pik3r1*$^{-/-}$, *Pik3r2*$^{+/-}$) mice, also on a mixed background, which contain the albumin-Cre transgene, to produce the five groups used in this study.

### Quantitative Reverse Transcription PCR analysis

Total RNA was isolated from mouse tissues using an RNeasy kit (QIAGEN, Valencia, California). cDNA was prepared from 1 μg of RNA using the Advantage RT-PCR kit (BD Biosciences, Palo Alto, California) with random hexamer primers, according to manufacturer's instructions. The resulting cDNA was diluted 10-fold, and a 5 μl aliquot was used in a 20 μl PCR reaction (SYBR Green, PE Biosystems) containing primers at a concentration of 300 nM each. PCR reactions were run in triplicate and quantitated in the ABI Prism 7700 Sequence Detection System. Ct values were normalized to TATA box binding protein (TBP) expression, and results were expressed as a fold change of mRNA compared to the indicated control mice. Primers for *Pck1*, *G6Pc*, *Fbp1*, *Srebf1c*, and *Fasn* were described previously (Taniguchi et al., 2005). Primers for p85β were designed across exon 1 and exon 2 since exon 1 is deleted in *Pik3r2* knockout mice. The forward primer for p85β is CCCTTGGATG GATCTTCTGA and the reverse primer is TCCACCAGCTTCACCAGAAT.

### Metabolic studies

For glucose tolerance testing (GTT), blood samples were obtained at 0, 15, 30, 60, and 120 min after intraperitoneal injection of 2 g/kg dextrose. Insulin

tolerance tests were performed by injecting 1 U/kg insulin (Novolin, Novo Nordisk, Denmark) intraperitoneally, followed by blood collection at 0, 15, 30, and 60 min. The pyruvate challenge was performed by injected 2 g/kg of pyruvate (Sigma) intraperitoneally, with blood glucose measured at 0, 15, 30, and 60 min time points. Blood glucose values were determined using a One Touch II glucose monitor (Lifescan Inc., Milipitas, California). Serum insulin and leptin levels were measured by ELISA using mouse insulin as a standard (Crystal Chem Inc., Chicago, Illinois). Serum adiponectin levels were analyzed from diluted mouse serum (1/1000) and analyzed by an ELISA kit (Linco). Nonesterified free fatty-acid levels were measured from random fed mice using a kit from Wako Diagnostics. The serum levels of the liver enzymes, bilirubin, total protein albumin, and triglycerides were measured by Anilytics (Gaithersburg, Maryland).

### In vivo insulin signaling

Following an overnight fast, mice were anesthetized with 2,2,2-tribromoethanol in PBS (Avertin), and injected with 5 U of regular human insulin (Novolin, Novo Nordisk, Denmark) via the inferior vena cava. Five minutes after the insulin bolus, tissues were removed and frozen in liquid nitrogen. Immunoprecipitation and immunoblot analysis of insulin signaling molecules were performed using tissue homogenates prepared in a tissue homogenization buffer that contained 25 mM Tris-HCl (pH 7.4), 10 mM $Na_3VO_4$, 100 mM NaF, 50 mM $Na_4P_2O_7$, 10 mM EGTA, 10 mM EDTA, 2 mM phenylmethylsulfonyl fluoride, 1% Nonidet-P40 supplemented with the Complete protease inhibitor cocktail (Roche). All protein expression data were quantified by densitometry using NIH Image.

### Antibodies

Rabbit polyclonal anti-IRS-1 antibody (IRS-1), anti-IRS-2 antibody (IRS-2), anti-IR antibody (IR), and pan-p85α antibody were generated as described previously (Ueki et al., 2002). Rabbit polyclonal anti-Akt, anti-phospho Akt (S473), anti-phospho FoxO1, anti-phospho GSK3β (Ser9), anti-FoxO1, anti-GSK3, anti-phosphoTSC2 (Thr1462), anti-TSC2, anti-phospho S6 (Ser240/244), and anti-S6 antibodies were purchased from Cell Signaling Technology (Beverly, Massachusetts). Myc-tag and isoform-specific Akt antibodies were purchased from Upstate Biotechnology (Lake Placid, New York). A polyclonal antibody for Westerns and immunoprecipitation against PKCλ/ζ was purchased from Santa Cruz Biotechnology.

### $PIP_3$ quantitation

Phosphatidylinositol(3,4,5)-triphosphate ($PIP_3$) levels were measured by a monoclonal antibody (IgM, Echelon Biosciences) as described previously (Kitamura et al., 2004), with a few modifications. Following insulin or saline treatment, mice were fixed by cardiac perfusion of 10% buffered formalin. The livers were then dehydrated in 30% sucrose overnight, then frozen in OCT compound (Sakura) for sectioning. For quantification of the immunofluorescence, four representative slides were chosen from each mouse and the fluorescence intensity of 16 fields per slide was measured and analyzed with VH-H1A5 analyzer software (KEYENCE, Osaka, Japan).

### In vitro kinase assays

Livers were extracted into tissue homogenization buffer and subjected to immunoprecipitation with IRS-1, IRS-2, or pTyr for PI3K assays as described previously (Taniguchi et al., 2005). Isoform-specific Akt antibodies were used to immunoprecipitate Akt1 or Akt2 from liver lysates then were subjected to Crosstide assay as described previously (Sakamoto et al., 2002). Reactions for atypical PKC activity were performed as reported previously (Sajan et al., 2004).

### Statistics

Data are presented as ± SEM. Student's t test was used for statistical analysis between two groups, while statistical significance between multiple treatment groups was determined by analysis of variance (ANOVA) and Tukey's t test. The trapezoid method was used to calculate area under the curve for ITT and GTT curves (Tran et al., 1996).

### Supplemental data

Supplemental data include one table and can be found with the article online at http://www.cellmetabolism.org/cgi/content/full/3/5/343/DC1/.

### Acknowledgments

We greatly appreciate the technical assistance of Laureen Mazzola and Will Wisdom. This work was supported by National Institutes of Health Grants DK33201 and DK55545, Joslin Diabetes and Endocrinology Research Center Grant DK34834 (to C.R.K.), and a GM41890 and CA089021 for L.C.C. C.M.T. acknowledges support from the American Diabetes Association Medical Scholars Award (C.M.T.) and a Medical Scientist Training Program scholarship (Harvard Medical School). J.L. acknowledges support from a HHMI predoctoral fellowship.

Received: December 22, 2005
Revised: March 22, 2006
Accepted: April 14, 2006
Published: May 9, 2006

### References

Bi, L., Okabe, I., Bernard, D.J., Wynshaw-Boris, A., and Nussbaum, R.L. (1999). Proliferative defect and embryonic lethality in mice homozygous for a deletion in the p110alpha subunit of phosphoinositide 3-kinase. J. Biol. Chem. *274*, 10963–10968.

Bi, L., Okabe, I., Bernard, D.J., and Nussbaum, R.L. (2002). Early embryonic lethality in mice deficient in the p110beta catalytic subunit of PI 3-kinase. Mamm. Genome *13*, 169–172.

Bruning, J.C., Michael, M.D., Winnay, J.N., Hayashi, T., Horsch, D., Accili, D., Goodyear, L.J., and Kahn, C.R. (1998). A muscle-specific insulin receptor knockout exhibits features of the metabolic syndrome of NIDDM without altering glucose tolerance. Mol. Cell *2*, 559–569.

Chen, G., Liang, G., Ou, J., Goldstein, J.L., and Brown, M.S. (2004). Central role for liver X receptor in insulin-mediated activation of Srebp-1c transcription and stimulation of fatty acid synthesis in liver. Proc. Natl. Acad. Sci. USA *101*, 11245–11250.

Cho, H., Mu, J., Kim, J.K., Thorvaldsen, J.L., Chu, Q., Crenshaw, E.B., 3rd, Kaestner, K.H., Bartolomei, M.S., Shulman, G.I., and Birnbaum, M.J. (2001). Insulin resistance and a diabetes mellitus-like syndrome in mice lacking the protein kinase Akt2 (PKB beta). Science *292*, 1728–1731.

Cross, D.A., Alessi, D.R., Cohen, P., Andjelkovich, M., and Hemmings, B.A. (1995). Inhibition of glycogen synthase kinase-3 by insulin mediated by protein kinase B. Nature *378*, 785–789.

Farese, R.V., Sajan, M.P., and Standaert, M.L. (2005). Atypical protein kinase C in insulin action and insulin resistance. Biochem. Soc. Trans. *33*, 350–353.

Fleischmann, M., and Iynedjian, P.B. (2000). Regulation of sterol regulatory-element binding protein 1 gene expression in liver: role of insulin and protein kinase B/cAkt. Biochem. J. *349*, 13–17.

Fruman, D.A., Mauvais-Jarvis, F., Pollard, D.A., Yballe, C.M., Brazil, D., Bronson, R.T., Kahn, C.R., and Cantley, L.C. (2000). Hypoglycaemia, liver necrosis and perinatal death in mice lacking all isoforms of phosphoinositide 3-kinase p85 alpha. Nat. Genet. *26*, 379–382.

Harris, T.E., and Lawrence, J.C., Jr. (2003). TOR signaling. Sci. STKE *2003*, re15.

Jiang, Z.Y., Zhou, Q.L., Coleman, K.A., Chouinard, M., Boese, Q., and Czech, M.P. (2003). Insulin signaling through Akt/protein kinase B analyzed by small interfering RNA-mediated gene silencing. Proc. Natl. Acad. Sci. USA *100*, 7569–7574.

Kitamura, T., Kitamura, Y., Nakae, J., Giordano, A., Cinti, S., Kahn, C.R., Efstratiadis, A., and Accili, D. (2004). Mosaic analysis of insulin receptor function. J. Clin. Invest. *113*, 209–219.

Kotani, K., Ogawa, W., Matsumoto, M., Kitamura, T., Sakaue, H., Hino, Y., Miyake, K., Sano, W., Akimoto, K., Ohno, S., and Kasuga, M. (1998). Requirement of atypical protein kinase clambda for insulin stimulation of glucose uptake but not for Akt activation in 3T3-L1 adipocytes. Mol. Cell. Biol. *18*, 6971–6982.

Luo, J., McMullen, J.R., Sobkiw, C.L., Zhang, L., Dorfman, A.L., Sherwood, M.C., Logsdon, M.N., Horner, J.W., Depinho, R.A., Izumo, S., and Cantley, L.C. (2005). Class IA phosphoinositide 3-kinase regulates heart size and physiological cardiac hypertrophy. Mol. Cell. Biol. *25*, 491–502.

Matsumoto, M., Ogawa, W., Akimoto, K., Inoue, H., Miyake, K., Furukawa, K., Hayashi, Y., Iguchi, H., Matsuki, Y., Hiramatsu, R., et al. (2003). PKClambda in liver mediates insulin-induced SREBP-1c expression and determines both hepatic lipid content and overall insulin sensitivity. J. Clin. Invest. *112*, 935–944.

Michael, M.D., Kulkarni, R.N., Postic, C., Previs, S.F., Shulman, G.I., Magnuson, M.A., and Kahn, C.R. (2000). Loss of insulin signaling in hepatocytes leads to severe insulin resistance and progressive hepatic dysfunction. Mol. Cell *6*, 87–97.

Ono, H., Shimano, H., Katagiri, H., Yahagi, N., Sakoda, H., Onishi, Y., Anai, M., Ogihara, T., Fujishiro, M., Viana, A.Y., et al. (2003). Hepatic Akt activation induces marked hypoglycemia, hepatomegaly, and hypertriglyceridemia with sterol regulatory element binding protein involvement. Diabetes *52*, 2905–2913.

Postic, C., and Magnuson, M.A. (2000). DNA excision in liver by an albumin-Cre transgene occurs progressively with age. Genesis *26*, 149–150.

Potter, C.J., Pedraza, L.G., and Xu, T. (2002). Akt regulates growth by directly phosphorylating Tsc2. Nat. Cell Biol. *4*, 658–665.

Puigserver, P., Rhee, J., Donovan, J., Walkey, C.J., Yoon, J.C., Oriente, F., Kitamura, Y., Altomonte, J., Dong, H., Accili, D., and Spiegelman, B.M. (2003). Insulin-regulated hepatic gluconeogenesis through FOXO1-PGC-1alpha interaction. Nature *423*, 550–555.

Sajan, M.P., Standaert, M.L., Miura, A., Kahn, C.R., and Farese, R.V. (2004). Tissue-specific differences in activation of atypical protein kinase C and protein kinase B in muscle, liver, and adipocytes of insulin receptor substrate-1 knockout mice. Mol. Endocrinol. *18*, 2513–2521.

Sakamoto, K., Hirshman, M.F., Aschenbach, W.G., and Goodyear, L.J. (2002). Contraction regulation of Akt in rat skeletal muscle. J. Biol. Chem. *277*, 11910–11917.

Sakoda, H., Gotoh, Y., Katagiri, H., Kurokawa, M., Ono, H., Onishi, Y., Anai, M., Ogihara, T., Fujishiro, M., Fukushima, Y., et al. (2003). Differing roles of Akt and serum- and glucocorticoid-regulated kinase in glucose metabolism, DNA synthesis, and oncogenic activity. J. Biol. Chem. *278*, 25802–25807.

Shepherd, P.R., Withers, D.J., and Siddle, K. (1998). Phosphoinositide 3-kinase: the key switch mechanism in insulin signalling. Biochem. J. *333*, 471–490.

Shimomura, I., Bashmakov, Y., Ikemoto, S., Horton, J.D., Brown, M.S., and Goldstein, J.L. (1999). Insulin selectively increases SREBP-1c mRNA in the livers of rats with streptozotocin-induced diabetes. Proc. Natl. Acad. Sci. USA *96*, 13656–13661.

Standaert, M.L., Sajan, M.P., Miura, A., Kanoh, Y., Chen, H.C., Farese, R.V., Jr., and Farese, R.V. (2004). Insulin-induced activation of atypical protein kinase C, but not protein kinase B, is maintained in diabetic (ob/ob and Goto-Kakazaki) liver. Contrasting insulin signaling patterns in liver versus muscle define phenotypes of type 2 diabetic and high fat-induced insulin-resistant states. J. Biol. Chem. *279*, 24929–24934.

Taniguchi, C.M., Ueki, K., and Kahn, R. (2005). Complementary roles of IRS-1 and IRS-2 in the hepatic regulation of metabolism. J. Clin. Invest. *115*, 718–727.

Taniguchi, C.M., Emanuelli, B., and Kahn, C.R. (2006). Critical nodes in signalling pathways: insights into insulin action. Nat. Rev. Mol. Cell Biol. *7*, 85–96.

Terauchi, Y., Tsuji, Y., Satoh, S., Minoura, H., Murakami, K., Okuno, A., Inukai, K., Asano, T., Kaburagi, Y., Ueki, K., et al. (1999). Increased insulin sensitivity and hypoglycaemia in mice lacking the p85 alpha subunit of phosphoinositide 3-kinase. Nat. Genet. *21*, 230–235.

Tran, T.T., Medline, A., and Bruce, W.R. (1996). Insulin promotion of colon tumors in rats. Cancer Epidemiol. Biomarkers Prev. *5*, 1013–1015.

Ueki, K., Algenstaedt, P., Mauvais-Jarvis, F., and Kahn, C.R. (2000). Positive and negative regulation of phosphoinositide 3-kinase-dependent signaling pathways by three different gene products of the p85alpha regulatory subunit. Mol. Cell. Biol. *20*, 8035–8046.

Ueki, K., Yballe, C.M., Brachmann, S.M., Vicent, D., Watt, J.M., Kahn, C.R., and Cantley, L.C. (2002). Increased insulin sensitivity in mice lacking p85beta subunit of phosphoinositide 3-kinase. Proc. Natl. Acad. Sci. USA *99*, 419–424.

Ueki, K., Fruman, D.A., Yballe, C.M., Fassaur, M., Klein, J., Asano, T., Cantley, L.C., and Kahn, C.R. (2003). Positive and negative roles of p85alpha and p85beta regulatory subunits of phosphoinositide 3-kinase in insulin signaling. J. Biol. Chem. *278*, 48453–48466.

Zhang, X., Gan, L., Pan, H., Guo, S., He, X., Olson, S.T., Mesecar, A., Adam, S., and Unterman, T.G. (2002). Phosphorylation of serine 256 suppresses transactivation by FKHR (FOXO1) by multiple mechanisms. Direct and indirect effects on nuclear/cytoplasmic shuttling and DNA binding. J. Biol. Chem. *277*, 45276–45284.